

1 Cardiotoxicity adverse outcome pathway network: 2 towards mechanistic and quantitative modelling

3
4 **Authors:** Luiz Ladeira¹, Devon A. Barnes², Rosalinde Masereeuw², Liesbet Geris^{1, 3, 4§}, Bernard
5 Staumont^{1§}

6 7 **Affiliations**

- 8 1. Biomechanics Research Unit, GIGA Institute, University of Liège, Belgium;
9 2. Utrecht University, Division of Pharmacology, Utrecht Institute for Pharmaceutical Sciences, Utrecht,
10 Netherlands;
11 3. Skeletal Biology and Engineering Research Center, KU Leuven, Belgium;
12 4. Biomechanics Section, Department of Mechanical Engineering, KU Leuven, Belgium.

13
14 Correspondence: Luiz Ladeira, lcladeira@uliege.be, Liesbet Geris, liesbet.geris@uliege.be, and Bernard
15 Staumont, b.staumont@uliege.be. Biomechanics Research Unit, GIGA Institute, University of Liège, Belgium

16
17 § Bernard Staumont and Liesbet Geris share senior authorship.

18 19 **ORCID**

20 Luiz Ladeira (0000-0002-7152-2688)
21 Devon A. Barnes (0000-0003-2037-2824)
22 Rosalinde Masereeuw (0000-0002-1560-1074)
23 Bernard Staumont (0000-0003-3155-4885)
24 Liesbet Geris (0000-0002-8180-1445)

31 **Plain language summary**

32
33 Why this study matters: Determining if a chemical or drug will damage the heart is a major
34 challenge in safety testing and impacts drug development. Traditionally, researchers look at
35 the final stages of heart damage, often missing the early warning signs. In this study, we
36 created a digital map that shows the "chain reaction" of events, starting from a chemical
37 interaction in the body and leading all the way to heart failure.

38 What we did: By gathering data from a global scientific database, we built a network of 64
39 biological events that lead to heart toxicity. Our map identifies "biological crossroads", which
40 are specific moments like cell stress or power failures within the cell, where many different
41 toxic chemicals converge to cause damage. We also describe how other organs, like the
42 kidneys, play an important role in how the heart reacts to these chemicals.

43 The impact: We made this map available in an easy-to-use website and provided a
44 catalogue of testing methods. This resource helps scientists design new, animal-free tests by
45 focusing on the most important biological signs of danger. Ultimately, this can potentially
46 make drug and other chemical developments safer by catching heart risks much earlier than
47 before.

48 **Abstract**

49

50 Chemical-induced heart toxicity remains a major challenge in drug development and
51 environmental safety, largely because current testing often relies on narrow, late-stage
52 endpoints that miss the complex biological progression of the toxicities. To address this, we
53 developed a comprehensive Adverse Outcome Pathway (AOP) network that maps how early
54 (bio)chemical triggers evolve into organ-level dysfunction. By integrating data from the
55 OECD AOP-Wiki, we constructed a unified network of 64 biological events and 94
56 documented relationships that identifies the critical biological "crossroads" where different
57 toxic chemicals converge to cause heart damage. Our analysis reveals a compact core of
58 central biological events, such as oxidative stress and mitochondrial dysfunction, which act
59 as the primary drivers of cardiac injury. This network approach moves beyond single, linear
60 pathways to show how systemic factors, including interactions with other organs like the
61 kidneys, contribute to cardiotoxicity. To translate these findings into a practical resource for
62 the broader scientific community, we developed a methods catalogue that links these
63 biological events to specific laboratory assays. To ensure this work is accessible and
64 actionable, we hosted the network on an interactive, FAIR-aligned web platform. By
65 providing a clear scaffold for understanding heart safety, this resource enables the design of
66 more human-relevant, animal-free testing strategies and helps prioritize the most impactful
67 biomarkers for future safety assessments.

68 **Keywords:**

69 Cardiac safety; adverse outcome pathways; toxicity; systems biology; next-generation risk
70 assessment.

71

72 **1. Introduction**

73 Cardiovascular diseases remain the leading cause of mortality worldwide (Global Burden of
74 Cardiovascular Diseases and Risks 2023 Collaborators, 2025; OECD, 2025), with
75 chemical-induced cardiotoxicity representing a significant and growing concern across both
76 therapeutic and environmental contexts (Daley et al., 2022; Georgiadis et al., 2022).
77 Mechanistically, cardiotoxicity arises from a diverse range of perturbations, including
78 mitochondrial dysfunction, oxidative stress, calcium mishandling, inflammation, and
79 disruption of ion homeostasis, ultimately leading to cardiac muscle damage. These
80 processes are not only biologically complex but also temporally variable, with adverse
81 outcomes manifesting over timescales ranging from seconds to decades (Mamoshina et al.,
82 2021). This variability poses a significant challenge for traditional detection methods,
83 primarily focusing on functional endpoints, such as contractility and hERG inhibition, which
84 often fail to capture the full spectrum of cardiotoxic effects (Daley et al., 2022). Such
85 limitation contributes to high attrition rates in pharmaceutical development and persistent
86 gaps in evaluating environmental chemicals (Daley et al., 2022; Mamoshina et al., 2021).

87 Beyond the pharmaceutical context, environmental cardiotoxicity has gained increasing
88 attention as a public health concern, with mounting evidence linking cardiovascular
89 dysfunction to chronic exposure to pollutants such as airborne particulates, pesticides, and
90 endocrine-disrupting chemicals (Daley et al., 2022; Georgiadis et al., 2022; Schaffert et al.,
91 2023). Despite this, cardiotoxicity remains unclassified as an independent hazard category in

92 regulatory frameworks, limiting recognition and hindering the development of tailored
93 assessment strategies (Georgiadis et al., 2022). Epidemiological data suggest that 7–23% of
94 the cardiovascular disease burden may be attributable to environmental exposures, yet the
95 underlying toxicological mechanisms remain insufficiently characterised (Daley et al., 2022).
96 Modern *in vitro* and *in silico* models, while promising, often focus on a limited spectrum of,
97 however relevant, targets, such as ion channels, failing to capture the broader mechanistic
98 landscape necessary for understanding cardiotoxicity (Daley et al., 2022). This systemic lack
99 of mechanistic understanding underscores the urgent need for more comprehensive,
100 mechanism-based approaches (Bajard et al., 2023) bridging effective protective strategies
101 and regulatory frameworks for both pharmaceutical and environmental chemical safety.

102 To address these challenges, mechanism-based frameworks are needed to complement
103 functional screening and enhance predictive resolution. The Adverse Outcome Pathway
104 (AOP) framework offers a conceptual construct designed to transform toxicity testing and
105 accelerate evidence-based risk assessment by leveraging data from multiple sources. An
106 AOP is defined as a sequence of measurable key events (KE), starting from a molecular
107 initiating event (MIE) and leading towards an adverse outcome (AO), connected via key
108 event relationships (KERs), which provide the scientific foundation for causal inferences
109 (Ankley et al., 2009; OECD, 2018; Vinken et al., 2017). It provides a structured,
110 stressor-agnostic way to organise existing mechanistic knowledge (Vinken et al., 2017).
111 AOPs delineate causal sequences of disturbed events across molecular, cellular, tissue, and
112 organ scales that ultimately produce adverse health or ecotoxicological outcomes at the
113 individual or population level (Ankley et al., 2009). Their modular architecture enables reuse
114 and recombination of KEs across pathways, supporting both knowledge integration and
115 systematic application. Although AOPs are typically developed as linear constructs,
116 combining them into networks better reflects the complexity of biological systems (Knapen et
117 al., 2018; Villeneuve et al., 2014) which makes them especially valuable for capturing
118 multiscale mechanisms such as multi-organ cross-talks.

119 The AOP-Wiki, developed and maintained under the oversight of the Organisation for
120 Economic Cooperation and Development (OECD), constitutes the primary public platform for
121 AOP development and dissemination (OECD, 2017, 2018). It structures mechanistic
122 knowledge grounded in expert curation and community contributions. Recent assessments
123 have revealed notable gaps and imbalances in the coverage of biological domains, with
124 cardiovascular mechanisms under-represented despite their regulatory relevance (Jaylet et
125 al., 2024). In particular, KEs such as oxidative stress and related processes, central to
126 cardiotoxicity, are inconsistently annotated or insufficiently linked to downstream outcomes.
127 Recent efforts have addressed these gaps by promoting harmonised KE terminology,
128 advancing data-driven mapping approaches (Mortensen et al., 2022, 2025; Tanabe et al.,
129 2022, 2023; Wittwehr et al., 2023, 2025).

130 Extending this approach to the heart requires adapting established network-based
131 methodologies to the specific mechanistic landscape of cardiotoxicity. The
132 cardiotoxicity-focused network presented in this work builds on the modular structure of the
133 AOP-Wiki to integrate dispersed information into a coherent and biologically relevant
134 network. To our knowledge, this is the first network-level integration of AOP-Wiki resources,
135 specifically focused on cardiotoxicity, providing a systematic map of how chemical-induced
136 events propagate to cardiac outcomes. The resulting representation facilitates the
137 identification of recurrent KEs across different contexts, highlighting shared mechanisms and

138 systemic contributors, such as cardio-renal interactions. These cross-cutting events are not
139 merely descriptive, as they are prioritised through network topological metrics to inform
140 assay selection, identify mechanistic gaps, and support the development of quantitative
141 models for predictive toxicology. This resource therefore represents both a conceptual and
142 operational advance, offering a foundational scaffold for integrating existing data, designing
143 test batteries, and anchoring new methods to clinically relevant mechanisms. Prior
144 applications in liver, kidney, endocrine and nervous system toxicology have demonstrated
145 the utility of this strategy in identifying mechanistically anchored, measurable and biologically
146 relevant KEs (Arnesdotter et al., 2021; Barnes et al., 2024; Spinu et al., 2019; Wiklund et al.,
147 2023). In this study, we apply a transparent screening and curation workflow to the AOP-Wiki
148 to assemble and characterise an AOP network for cardiotoxicity, with the goal of identifying
149 relevant KEs as a foundation for future animal-free and human-relevant quantitative *in vitro*
150 and *in silico* toxicity predictions.

151

152 2. Methods

153 We built a data-driven AOP network following already established methods (Arnesdotter et
154 al., 2021; Barnes et al., 2024; Spinu et al., 2019; Wiklund et al., 2023). Briefly, it includes
155 definition of purpose, data collection and screening process, inclusion and exclusion criteria,
156 data curation and harmonisation, and network building, followed by a comprehensive
157 analysis as previously described (Villeneuve et al., 2014). We also mapped the KE
158 quantification methods reported at AOP-Wiki and built an interactive catalogue that can be
159 displayed in an interactive version of the network, as described in the sections below.

160

161 2.1 Definition of purpose

162 This study aimed to identify, describe, and investigate the mechanisms of cardiotoxicity
163 caused by chemical stimuli previously documented in the AOP-Wiki database. AOPs
164 describing cardiotoxicity and the KEs associated with cardiotoxic mechanisms were
165 integrated into an AOP network and analysed to better understand the relationships between
166 MIEs and adverse outcomes in the heart.

167

168 2.2 Data collection and screening process

169 A manual search of the AOP-Wiki (<https://aopwiki.org/>) was conducted on August 12, 2025,
170 to identify individual AOPs concerning cardiotoxicity. The Key Events dataset was
171 downloaded (https://aopwiki.org/downloads/aop_ke_mie_ao.tsv) and searched for KEs and
172 AOs associated with cardiotoxicity using the following keywords: "heart", "cardio", "cardiac",
173 "ventricular", "ventricle", "myocardial", "myocardium", "atrial", "atrio", and "atrium"
174 (Supplementary Data S1).

175 We intentionally excluded vascular-related keywords from the KEs screening because this
176 study focused specifically on toxicological mechanisms primarily affecting cardiac tissue and
177 function. While vascular dysfunction can secondarily influence the heart, such mechanisms
178 fall outside the defined scope of this network, which targets MIEs and KEs with a direct
179 mechanistic link to the heart. As is evident in the results, some vascular-related or other

180 non-myocardium-related KEs are present in the final network, which can be justified for their
181 presence in larger and cross-organ AOPs selected based on the inclusion/exclusion criteria.

182 This initial search identified 19 AOPs containing KEs related to cardiotoxicity: AOP:16,
183 AOP:21, AOP:94, AOP:104, AOP:138, AOP:150, AOP:177, AOP:186, AOP:261, AOP:304,
184 AOP:377, AOP:426, AOP:427, AOP:433, AOP:436, AOP:456, AOP:479, AOP:480, and
185 AOP:539. A subsequent manual search for AOP titles using the same keywords directly on
186 the database identified three additional AOPs: AOP:438, AOP:448, and AOP:515.

187

188 2.3 Inclusion and exclusion criteria

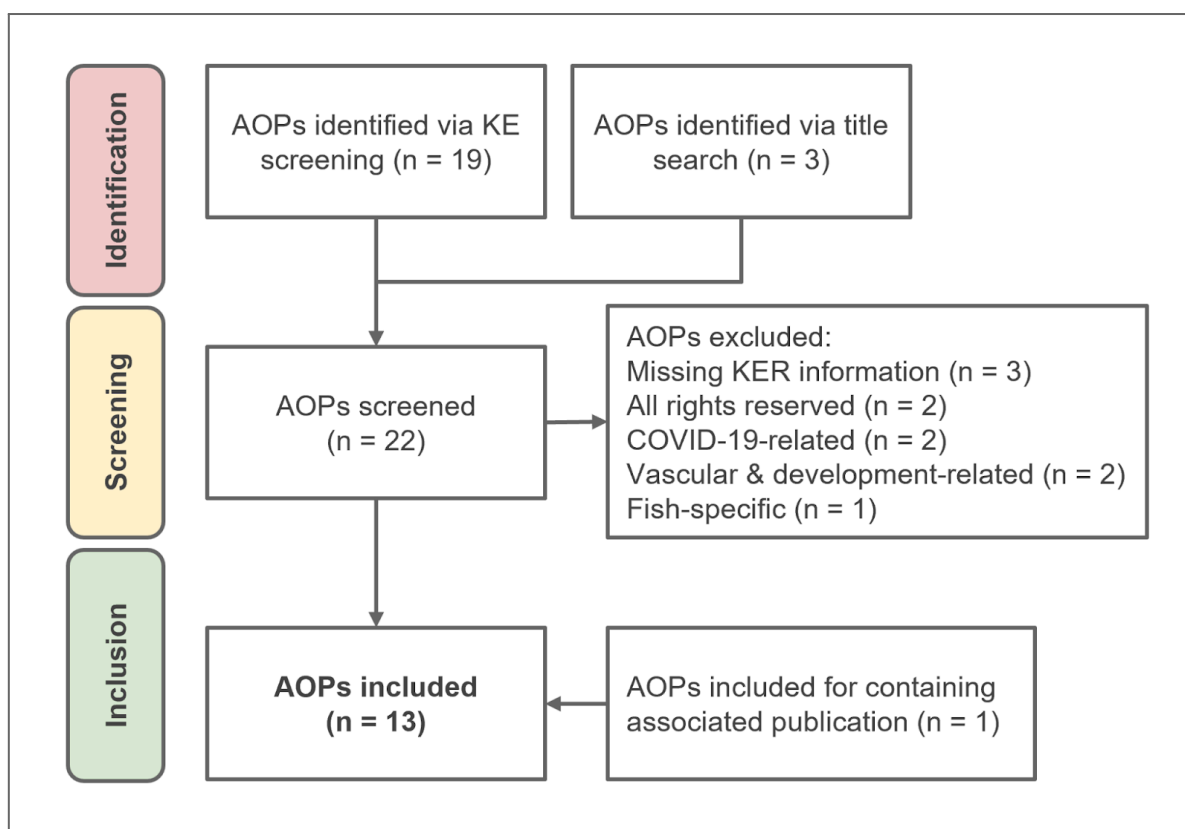
189 AOPs were assessed and included based on the presence of a cardiotoxicity-related key
190 event (KE) or adverse outcome (AO). AOPs were excluded based on the following criteria:

- 191 ● Lack of KER information (n = 3): AOP:186, AOP:377, AOP:448.
- 192 ● All rights reserved & no permission granted (n = 2): AOP:438, AOP:515.
- 193 ● COVID-19-related (n = 2): AOP:426, AOP:427.
- 194 ● Vasculature & development-related (n = 2): AOP:304, AOP:436.
- 195 ● Fish-specific (n=1): AOP:539.

196 Although other AOPs also include fish in their taxonomy domain, AOP:539 was the only one
197 among them specifically designed for freshwater fish species, including the “KE2236 -
198 Decreased, Sodium uptake in gills”, which led to its exclusion from the analysis. At the time
199 of this publication, no reuse permission was obtained from the AOPs with an “all rights
200 reserved” licence, leading to exclusion from the analysis.

201 Figure 1 illustrates the screening process. One AOP (AOP:448) was initially excluded due to
202 lack of KERs information in the AOP-Wiki database. However, a publication regarding this
203 AOP was identified, and it was subsequently re-included in the analysis. Supplementary
204 Data S2 contains an overview of the AOPs screened.

205



206

207 **Figure 1.** AOP-Wiki screening process for cardiotoxicity-related Adverse Outcome
208 Pathways.

209

210 2.4 Key event harmonisation

211 To ensure consistency in the network analysis, Key Event (KE) titles with similar biological
212 meanings or functions were merged. Duplicated KEs were identified and grouped under
213 common terms. In addition, we standardised nomenclature with uppercase letters at the
214 beginning of the names and removed NA entries. The complete harmonised data can be
215 found in Supplementary Data S3.

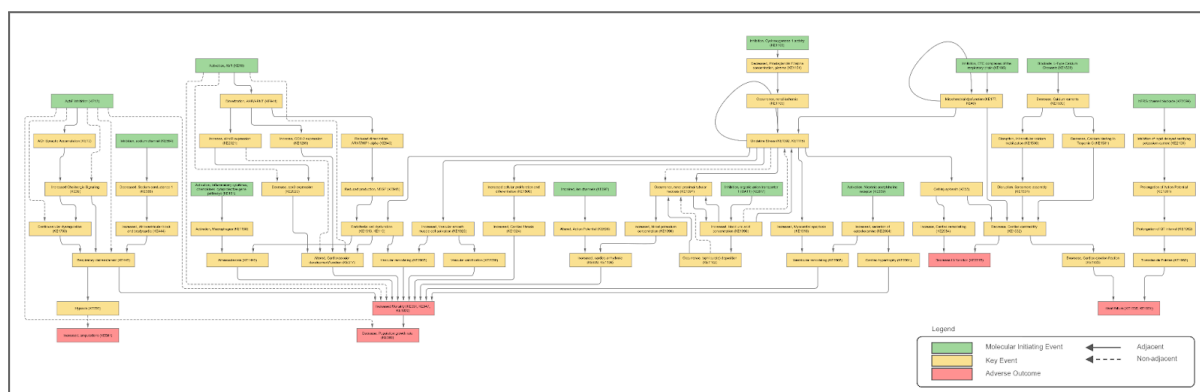
216 2.5 Network building and visualization

217 Next, AOP data was extracted manually from each entry and/or their related publications.
218 The data was consolidated in a spreadsheet and cleaned by keeping only the columns
219 necessary for data visualization and analysis (Supplementary Data S4 & S5), which was
220 used for the network building and subsequent analysis.

221

222 The AOP network was built using the open-source software platform Cytoscape (v. 3.10.4;
223 <https://cytoscape.org/>) (Shannon et al., 2003). The network was automatically organised
224 using the yFiles Hierarchic Layout algorithm. Additional annotations, including KE adjacency
225 (edge type – dotted or continuous) and type (node colour), were added to enhance the
226 clarity of the network's visual components. Supplementary Data S6 contains node attributes
227 and was used to support the visualisation generation. KEs were represented as nodes in the

228 network and classified as MIEs (green), KEs (yellow), or AOs (red). Adjacent Key Event
229 Relationships (KERs) were represented as directed continuous edges (connecting arrows),
230 and non-adjacent KERs were represented as directed dotted edges, linking upstream and
231 downstream KEs. The final network representation is shown in Figure 2.



233 **Figure 2.** Adverse Outcome Pathway network of 13 AOPs of cardiotoxicity available on the
234 AOP-Wiki as of August 12, 2025.

235

236 2.6 Network analysis

237 The distribution of node types was quantified to assess the proportional representation of
238 event types in the cardiotoxicity network. Node relationships were categorised according to
239 their adjacency (adjacent vs. non-adjacent) and the level of supporting evidence (high,
240 moderate, or unspecified). Evidence levels and the degree of quantitative understanding for
241 each relationship were extracted from AOP-Wiki entries and categorised accordingly. For
242 analysis purposes, evidence levels labelled as “High” or “Strong” were grouped under “High,”
243 while “Not Specified” and “NA” were consolidated under “Not Specified.”

244 The Cytoscape Network Analyzer tool was used to compute standard network metrics
245 considering a directed network. Several network metrics were calculated to identify critical
246 nodes. The betweenness centrality was calculated for each node to measure its importance
247 as a bridge connecting different parts of the network. Total degree (sum of in-degree and
248 out-degree) was calculated for each node to identify the most connected nodes in the
249 network. Stress centrality was calculated to identify critical convergence hubs, measuring the
250 total number of shortest paths passing through a node. A combined importance score was
251 computed by normalising and summing the above centrality measures to identify the overall
252 most critical nodes in the network.

253 Nodes were classified as convergent or divergent based on their connectivity patterns.
254 Convergent nodes were considered those with more incoming connections than outgoing
255 (in-degree > out-degree). On the contrary, divergent nodes are those with more outgoing
256 connections than incoming (out-degree > in-degree). This classification helped identify key
257 regulatory points and potential intervention targets within the cardiotoxicity network.

258 Overall network metric results can be found in Supplementary Data S7. A reproducible R
259 script for this analysis is provided in Supplementary Scripts.

260 The Pesca3.0 Cytoscape plugin (<https://apps.cytoscape.org/apps/pesca30>) was used to
261 compute the simple path occurrence (Scardoni et al., 2015), which represents a more
262 appropriate metric for betweenness centrality in the AOP network context (Barnes et al.,
263 2024). The distribution of path lengths within the network was analysed to assess network
264 compactness and efficiency in information flow. For each KE, simple path occurrence was
265 defined as the number of distinct MIE to AO simple paths in which the KE appears as an
266 internal node. This was visualised as a histogram showing the frequency of paths of different
267 lengths. Simple path metrics can be found in Supplementary Data S8.

268 2.7 Cataloguing methods for KE detection

269 A catalogue of detection methods was built by collecting and organising information
270 available at each KE unique page in AOP-Wiki, especially in the section “How It Is Measured
271 or Detected”. The section text from each KE was automatically retrieved from the latest
272 release of the AOP-Wiki XML database (version 2025-07-01) available at
273 <https://aopwiki.org/downloads/aop-wiki-xml-2025-07-01.gz>. We extracted the text for all KEs
274 present in our network (script provided in Supplementary Scripts), organised, checked
275 manually AOP-Wiki entries for missing data and summarised the information available in a
276 catalogue, which is available as Supplementary Data S9.

277

278 2.8 Interactive visualization of the AOP network and related data

279 Following the example of Mazein et al. (2025), we prepared an online interactive version of
280 the AOP network for user exploration and for network interoperability, reuse and sharing. For
281 this, an SBML representation of the AOP network was generated using a dedicated R script
282 based on the minervar package (Gawron et al., 2023). To this end, the network data were
283 pre-processed, annotated, and converted into a CellDesigner-compatible SBML format
284 (Funahashi et al., 2008). Due to CellDesigner constraints, the two self-loops present in the
285 network could not be represented in this interactive version. The network layout was then
286 manually curated within CellDesigner. Context annotations (e.g., biological level and organ-
287 or cell-type where the KE happens) were assigned to KEs in order to organise the network in
288 a context-specific manner, visualising KEs on top of the cells, organs, compartments, or
289 human-scale level. The context annotations can be found in Supplementary Data S6. The
290 final model was deployed on the MINERVA (Molecular Interaction NETwork VisuAlization)
291 platform (Hoksza et al., 2020) for interactive exploration and is accessible online at
292 <http://cardiotox.elixir-luxembourg.org/>.

293

294 To illustrate evidence levels and the degree of quantitative understanding for each KER,
295 annotations from AOP-Wiki were processed and visualised as overlays within MINERVA. A
296 reproducible R script for handling categorical data overlay is provided in Supplementary
297 Scripts. This script formats data according to MINERVA’s overlay specifications, including
298 standardised headers with version information, descriptive labels, and descriptions. Output
299 files were exported as tab-separated text files compatible with MINERVA’s overlay
300 visualisation engine.

301

302 It is important to note that different data types may require tailored processing to optimise
303 visualisation within the MINERVA environment. Users are encouraged to consult the

304 MINERVA User Manual at <https://minerva.pages.uni.lu/doc/> for detailed guidance on creating
305 fit-for-purpose overlays.

306

307 Moreover, a MINERVA plugin (Hoksza et al., 2019) was prepared to dynamically map KE
308 detection methods to the displayed network. For that, a JavaScript plugin was designed to
309 access and display information from a Google Spreadsheet, map the information against the
310 nodes in the network and tag the nodes dynamically displayed in the plugin table. The data
311 source used is the catalogue of methods for KE detection built from AOP-Wiki entries. The
312 plugin source code can be accessed via
313 https://github.com/luiz-ladeira/cardiotox_aop_minerva_plugin and the plugin can be used in
314 the MINERVA platform by loading it with the following link:
315 [https://raw.githubusercontent.com/luiz-ladeira/cardiotox_aop_minerva_plugin/master/plugin.j](https://raw.githubusercontent.com/luiz-ladeira/cardiotox_aop_minerva_plugin/master/plugin.js)
316 [s](#).

317

318 2.9 Software

319 All the analyses were done using R version 4.4.0 (2024-04-24 ucrt) (R Core Team, 2024)
320 and R Studio version 2023.12.1.402 (Ocean Storm) (Posit team, 2024). Visualisation of the
321 network was generated using Cytoscape version 3.10.4 (Shannon et al., 2003) and graphs
322 were generated using ggplot2 (Wickham, 2016). The network layout was curated in
323 CellDesigner version 4.4 (Funahashi et al., 2008). Interactive visualisation is provided using
324 the MINERVA platform version 19 (Hoksza et al., 2019). All scripts are provided in
325 Supplementary Scripts.

326

327 3. Results

328 3.1 Assembling the cardiotoxicity AOP network

329 A total of 22 linear AOPs were initially identified through a manual AOP-Wiki search and title
330 screening (Figure 1). After applying the predefined inclusion and exclusion criteria, 13 AOPs
331 were retained for inclusion in the cardiotoxicity network (Supplementary Data S2). These
332 selected AOPs reflect a diverse array of initiating mechanisms and AOs relevant to cardiac
333 toxicity. MIEs included acetylcholinesterase inhibition (AOP:16), aryl hydrocarbon receptor
334 (AhR) activation (AOPs:21, 150, 456), ion channel perturbations such as sodium channel
335 inhibition and hERG channel blockade (AOPs:94, 104, 433), and inhibition of mitochondrial
336 electron transport chain complexes (AOPs:479, 480). The resulting AOs ranged from
337 non-specific endpoints like increased mortality to more organ-specific manifestations such as
338 decreased left ventricular function, heart failure, and sudden cardiac death. Three AOPs
339 (AOPs:21, 150, 456) have received OECD endorsement or are currently under review, while
340 the remaining are still under development or have not yet undergone formal evaluation.

341 Although AOP:433 targets “sudden cardiac death” in AOP-Wiki, during KE harmonisation
342 this outcome was consolidated under “Heart failure (KE1535, KE1964)” to avoid duplication
343 and maintain a compact AO layer (Supplementary Data S3). AOP:448 was included despite
344 lacking formally defined MIE and AO annotations in the AOP-Wiki, as its structure and

345 mechanistic components are comprehensively described in an associated peer-reviewed
346 publication (Ding et al., 2022). Similarly, additional AOPs included in the network are
347 supported by published literature that complements or expands upon the information
348 available in the AOP-Wiki. For instance, the current status of AOP:16 on AOP-Wiki is “under
349 development” but has its mechanistic basis and key relationships detailed in a published
350 article (Russom et al., 2014), while AOPs:21 and 150 are both OECD-endorsed and
351 described in formal OECD Series reports (Amani Farhat & Sean W. Kennedy, 2019; Jon
352 Doering et al., 2019). AOP:456, which is currently “under review” on the database, is also
353 accompanied by a peer-reviewed article providing additional context and evidence (Shankar
354 & Villeneuve, 2023). These publications enriched the datasets by providing mechanistic
355 detail, empirical evidence, and contextual information that, in some cases, were not fully
356 captured in the AOP-Wiki entries alone.

357 An overview of the AOPs represented in the final network, as recorded in the AOP-Wiki at
358 the time of the data collection, is provided in Table 1.

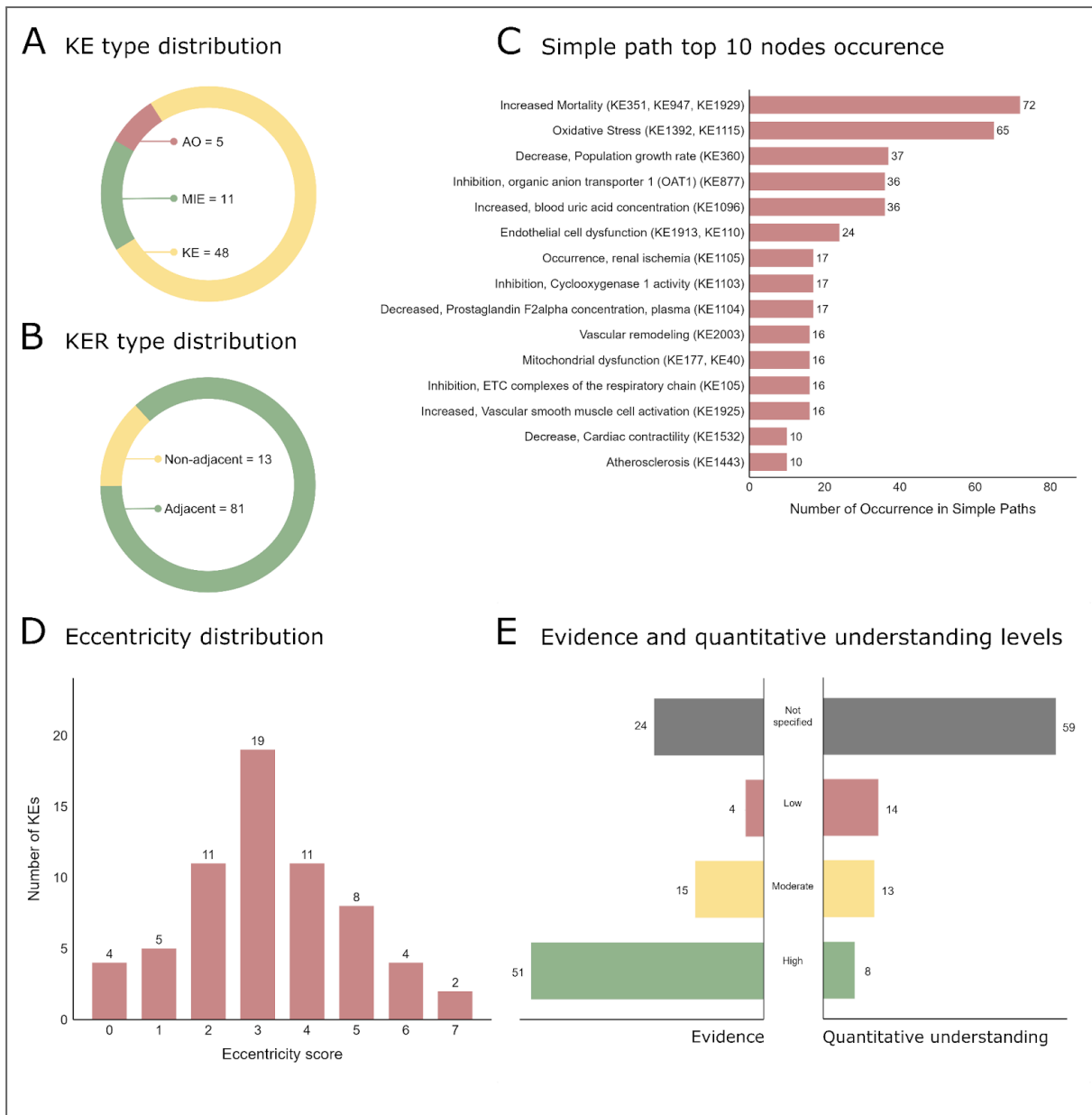
359 **Table 1.** Adverse Outcome Pathways extracted from AOP-Wiki to compose the cardiotoxicity
360 AOP network. MIE: Molecular Initiating Event. AO: Adverse Outcome. OECD Organisation
361 for Economic Co-operation and Development.

ID	Title	MIE	AO	OECD status	Available at:
16	Acetylcholinesterase inhibition leading to acute mortality	Acetylcholinesterase (AChE) Inhibition	Increased Mortality; Decrease, Population growth rate	Under Development	https://aopwiki.org/aops/16
21	Aryl hydrocarbon receptor activation leading to early life stage mortality, via increased COX-2	Activation, AhR	NA	WPHA/WNT Endorsed	https://aopwiki.org/aops/21
94	Sodium channel inhibition leading to congenital malformations	Inhibition, sodium channel	Increased, amputations	NA	https://aopwiki.org/aops/94
138	Organic anion transporter (OAT1) inhibition leading to renal failure and mortality	Inhibition, organic anion transporter 1 (OAT1)	Increased Mortality; Decrease, Population growth rate	NA	https://aopwiki.org/aops/138
104	Altered ion channel activity leading to impaired heart function	Impaired, ion channels	Increased Mortality	NA	https://aopwiki.org/aops/104
150	Aryl hydrocarbon receptor activation leading to early life stage mortality, via reduced VEGF	Activation, AhR	Increase, Early Life Stage Mortality	WPHA/WNT Endorsed	https://aopwiki.org/aops/150
177	Cyclooxygenase 1 (COX1) inhibition leading to renal failure and mortality	Inhibition, Cyclooxygenase 1 activity	Increased Mortality; Decrease, Population growth rate	NA	https://aopwiki.org/aops/177
261	L-type calcium channel blockade leading to heart failure via decrease in cardiac contractility	Blockade, L-Type Calcium Channels	Heart failure	Under Development	https://aopwiki.org/aops/261
433	hERG channel blockade leading to sudden cardiac death	hERG channel blockade	Sudden cardiac death	NA	https://aopwiki.org/aops/433
448	ROS, inflammation, and activation of nAChR lead to increased incidence of cardiovascular morbidity and mortality	NA	NA	NA	https://aopwiki.org/aops/448

456	Aryl hydrocarbon receptor activation leading to early life stage mortality via sox9 repression induced cardiovascular toxicity	Activation, AhR	Increase, Early Life Stage Mortality	Under Review	https://aopwiki.org/aops/456
479	Mitochondrial complexes inhibition leading to left ventricular function decrease via increased myocardial oxidative stress	Inhibition, Mitochondrial Electron Transport Chain Complexes	Decrease Left Ventricular function	Under Development	https://aopwiki.org/aops/479
480	Mitochondrial complexes inhibition leading to heart failure via decreased ATP production	Inhibition, Mitochondrial Electron Transport Chain Complexes	Decrease Left Ventricular function	Under Development	https://aopwiki.org/aops/480

362

363 Following KE harmonisation, the final network included 64 nodes and 94 directed edges,
364 representing 11 MIEs, 48 KEs, and 5 AOs (Figure 3A). Adjacent KERs comprised 86.17%
365 (n=81) of all connections, while 13.83% (n=13) were non-adjacent links integrated to
366 preserve biological coherence across divergent AOP structures (Figure 3B). KE sharing was
367 predominantly skewed toward single-occurring nodes, yet a subset served as cross-cutting
368 integrators. Of the total 64 KEs, 47 (73,44%) appeared in a single AOP, 10 (15.63%) in two,
369 5 (7.81%) in three, and one each (1,56%) in four and eight AOPs. “Increased Mortality
370 (KE351, KE947, KE1929)” was the most recurrent (8 AOPs), followed by “Oxidative Stress
371 (KE1392, KE1115)” (4 AOPs). Clusters of KEs sharing three AOPs were observed along the
372 AhR axis (“Activation, AhR”; “Dimerization, AHR/ARNT”) and in cardiovascular function
373 (“Altered, Cardiovascular development/function”; “Decrease, Cardiac contractility”;
374 “Increased, cardiac arrhythmia”) (Supplementary Files).



375

376 **Figure 3.** Analysis summary of the cardiotoxicity AOP network. A - Key event type
 377 distribution. B - Key event relationship type distribution. C - Top 15 nodes by occurrence in
 378 simple paths. D - Eccentricity distribution. E - Evidence and quantitative understanding levels
 379 of adjacent and non-adjacent key event relationships. KE: Key events; KER: Key event
 380 relationship.

381

382 3.2 Structural and topological characterization

383 Analysis of the network structure demonstrated heterogeneous connectivity patterns with
 384 hubs that bridge multiple mechanistic domains. The total degree had a mean of 2.94 and a
 385 maximum of 13. The most connected nodes were "Oxidative Stress (KE1392, KE1115)" and
 386 "Increased Mortality (KE351, KE947, KE1929)", both with a total degree of 13 and 12
 387 respectively, followed by extra-cardiac integrators such as "Occurrence, renal proximal

388 tubular necrosis (KE1104)" in 3rd place and "Increased, blood uric acid concentration
 389 (KE1096)" in 7th place. These events acted as hubs, bridging multiple mechanistic domains
 390 within the cardiotoxicity cascade.

391 The betweenness centrality ranked "Oxidative Stress (KE1392, KE1115)" as the
 392 highest-betweenness node (1.23), followed by "Increased, blood uric acid concentration
 393 (KE1096)" (0.49), and "Decrease, Cardiac contractility (KE1532)" (0.39). These nodes lie on
 394 many of the shortest paths and are positioned to mediate communication between
 395 mechanistic modules. Interestingly, the second-positioned KE and other top-ranked ones in
 396 betweenness centrality occur outside the heart, in the kidneys, highlighting the systemic
 397 nature of cardiac physiology and the cardio-renal interdependence.

398 The stress centrality reached its maximum values for key integrative nodes, most notably
 399 "Oxidative Stress (KE1392, KE1115)", "Increased Mortality (KE351, KE947, KE1929)", and
 400 "Endothelial cell dysfunction (KE1913, KE110)". This pattern indicates that these nodes
 401 serve as critical convergence points for a vast number of adverse pathways, consistent with
 402 their roles as essential bridges between upstream initiators and downstream outcomes.

403 To capture multidimensional prominence, we computed a combined importance score. By
 404 this index, "Oxidative Stress (KE1392, KE1115)" ranked first, followed by "Increased
 405 Mortality (KE351, KE947, KE1929)", "Decrease, Cardiac contractility (KE1532)", "Endothelial
 406 cell dysfunction (KE1913, KE110)" and "Increased, blood uric acid concentration (KE1096)".
 407 These results indicate that oxidative stress and mortality function simultaneously as
 408 mechanistic hubs and critical outcomes within the network.

409 Complete data on the topographic indicators can be found in Supplementary Data S7.

410 Directional balance was investigated through convergent/divergent status (Table 2). We
 411 identified 14 (21.9%) convergent nodes (downstream recipients with larger inflow), 13
 412 (20.3%) divergent nodes (upstream initiators with larger outflow), and 37 (57.8%) balanced
 413 nodes.

414 **Table 2.** List of the identified convergent and divergent key events.

415

Convergent KEs		Divergent KEs	
Type	Name	Type	Name
AO	Increased Mortality	KE	Dimerization, AHR/ARNT
KE	Altered, Cardiovascular development/function	KE	Cell injury/death
KE	Occurrence, renal proximal tubular necrosis	KE	Decrease, Calcium currents
KE	Atherosclerosis	KE	Increase, slincR expression
KE	Cardiovascular dysregulation	KE	Increased, Vascular smooth muscle cell activation
AO	Decrease LV function	KE	Increased, blood uric acid concentration
KE	Decrease, Cardiac contractility	KE	Increased, secretion of catecholamine
AO	Decrease, Population growth rate	KE	Occurrence, tophi (urate) deposition

KE	Decrease, sox9 expression	KE	Oxidative Stress
AO	Heart failure	KE	Endothelial cell dysfunction
KE	Increased, cardiac arrhythmia	KE	Mitochondrial dysfunction
KE	Respiratory distress/arrest	MIE	AchE Inhibition
KE	Vascular remodeling	MIE	Activation, AhR
KE	Ventricular remodeling		

416

417 Regarding simple path occurrence, the analysis highlighted a small set of recurrent
 418 mediators. As shown in Figure 3C, the fifteen nodes with the highest counts included KEs
 419 taking place in the heart as "Oxidative Stress (KE1392, KE1115)", "Decrease, Cardiac
 420 contractility (KE1532)" and "Mitochondrial dysfunction (KE177, KE40)", as well as renal
 421 physiology-related KEs, such as "Increased, blood uric acid concentration (KE1096)" and
 422 "Occurrence, renal ischemia (KE1105)", among others. Top nodes are expected to recur
 423 across many mechanistic routes, consistent with their strategic positions along alternative
 424 trajectories. These findings suggest moderate network compactness and efficient signal
 425 propagation between MIEs and AOs across multiple mechanistic routes.

426 Eccentricity complements degree- and path-based centralities by quantifying the maximum
 427 distance from each key event to its farthest accessible downstream target. This index ranged
 428 from 0 to 7, with the majority of nodes clustered between scores of 2 and 4 (Figure 3D).
 429 Outcome-level nodes such as "Increased Mortality (KE351, KE947, KE1929)", "Decrease,
 430 Cardiac ejection fraction (KE1533)", "Increase, Cardiac remodelling (KE2084)" and
 431 "Torsades de Pointes (KE1963)", among others, showed low eccentricity. This low score
 432 confirms their topology as terminal or penultimate sink nodes, representing the endpoints of
 433 biological cascades. High-eccentricity nodes, such as "Occurrence, tophi (urate) deposition
 434 (KE1102)" and "Inhibition, Cyclooxygenase 1 activity (KE1103)" are peripheral initiators
 435 whose effects require multiple steps to reach the final adverse outcomes.

436 3.3 Key Event Relationships: Evidence and Quantitative Understanding

437 Assessment of KER evidence and quantitative understanding included adjacent and
 438 non-adjacent relationships for a broader evaluation of the network. Evidence levels revealed
 439 that 54.26% (n=51) were supported by high or strong evidence, 15.96% (n=15) had
 440 moderate support, 4.25% (n=4) presented low levels of evidence, while 25.53% (n=24)
 441 lacked specified evidence levels (Figure 3E). Similarly, the degree of quantitative
 442 understanding was limited, with only 37.2% (n=35) of KERs associated with any quantitative
 443 level of understanding. This highlights persistent gaps that may hinder mechanistic
 444 modelling and prediction efforts. Full distribution of these data is illustrated in Figure 3E.

445 These data were prepared as overlays for visualisation on the interactive network displayed
 446 in MINERVA, and can be accessed via the "Overlays" feature at
 447 https://ontox.elixir-luxembourg.org/minerva/index.html?id=cardiotox_aop. Figure 4B displays
 448 an example of how KER data - evidence levels in the figure - is visualised at the platform.

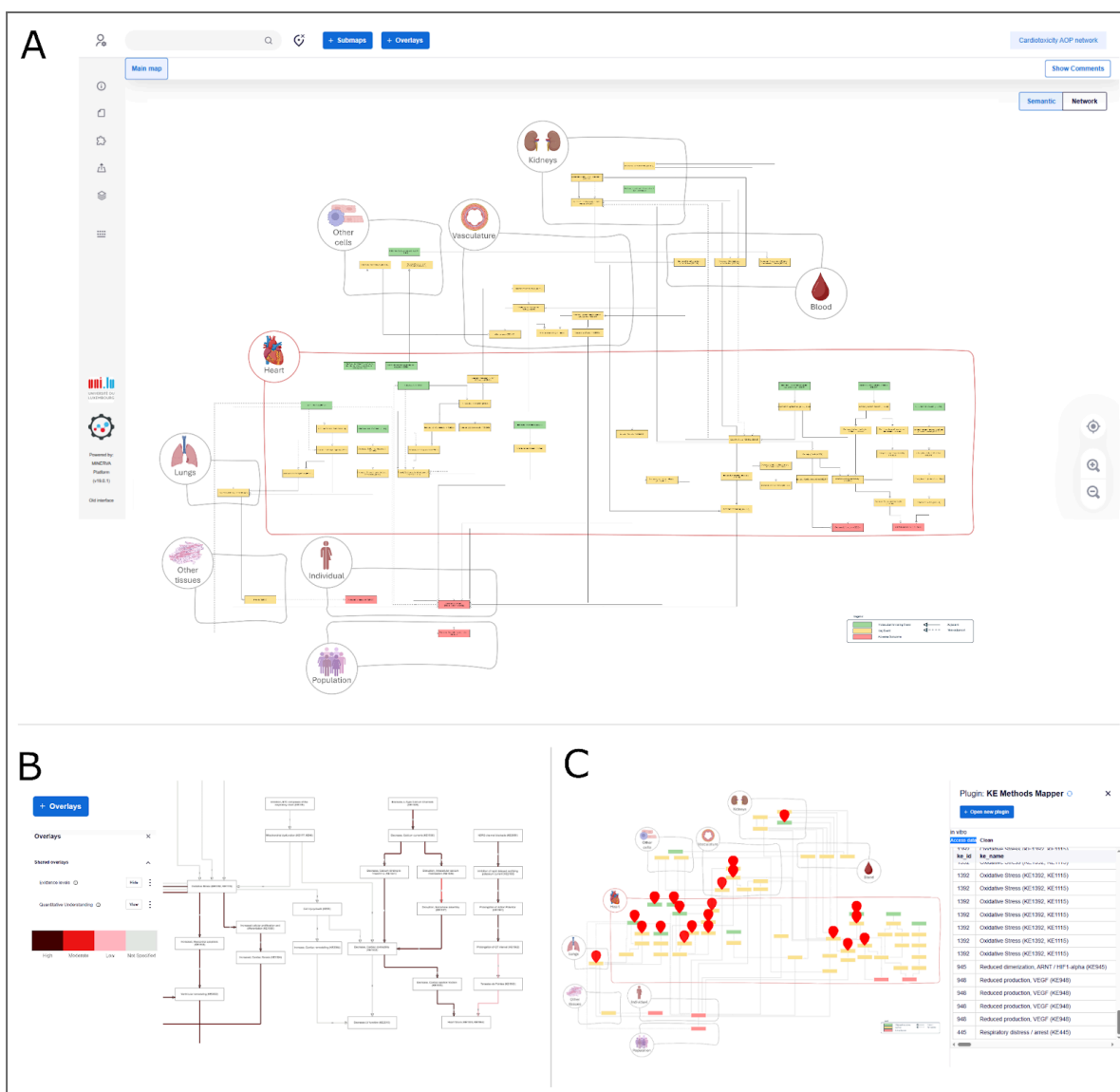
449 3.4 Cataloging KE measurement assays

450 By analysing the 71 unique KE ID entries (after harmonisation the total number of KEs was
451 64) on AOP-Wiki, we gathered the methods used to monitor or quantify the endpoints. Out of
452 the 64 unique KEs, 43.75% (n=28) had detection methods explicitly described in the
453 AOP-Wiki. These included *in vivo*, *in vitro* and *in silico* methodologies, such as biochemical
454 assays, imaging, electrophysiological recordings, and molecular biomarkers (Supplementary
455 Data S9). The first version of this catalogue is fully based on what AOP authors reported in
456 the KE entries and does not represent all the potential methods to quantify a KE. However,
457 as a living resource, it is subject to subsequent updates that will help fill the methodological
458 gaps in itself and potentially in AOP-Wiki. At this stage, it serves as a starting point for
459 developing an integrated test battery for cardiotoxicity assessment.

460 A MINERVA platform plugin (Figure 4C) was developed for dynamic visualisation and search
461 of methods for the KEs present in this network. It maps the catalogue on top of the network
462 and facilitates on-demand method mapping. The plugin and its source code can be found at
463 https://github.com/luiz-ladeira/cardiotox_aop_minerva_plugin. To use it, the user can load
464 the plugin directly at the MINERVA platform as described in the methods section.

465 3.5 Interactive Visualization and Contextual Annotations

466 The complete AOP network was made accessible through a MINERVA-based interactive
467 platform (https://ontox.elixir-luxembourg.org/minerva/index.html?id=cardiotox_aop). The two
468 self-loops (“Oxidative Stress” and “Mitochondrial dysfunction”) present in the network are not
469 represented in the interactive version due to CellDesigner software limitations. Nodes were
470 spatially organised according to biological scale (cellular, tissue, organ) related to their
471 contextual metadata (Supplementary Data S6). To improve clarity, an adaptation of the
472 Systems Biology Graphical Notation (SBGN) Activity Flow (AF) language (Mi et al., 2015;
473 Novère et al., 2009) was implemented, in which the rectangle shape represented a KE
474 (equivalent to Biological Activity in SBGN-AF), a directed solid arrow was used for adjacent
475 KERs, and a directed dotted arrow was used for non-adjacent KERs, indicating the flow of
476 information. Figure 4A shows an overview of the network as displayed in the MINERVA
477 platform.



478

479 **Figure 4.** Overview of the interactive cardiotoxicity AOP network model on the MINERVA
 480 platform. A - Overview of the platform displaying the network. B - Example of data overlay
 481 visualisation, highlighting different levels of evidence support to the key event relationships.
 482 C - KE Methods Mapper plugin overview, showing how the methods catalogue is mapped on
 483 the AOP network.

484

485 4. Discussion and conclusions

486 The AOP framework is a valuable tool for organising mechanistic knowledge to support
 487 chemical safety assessment, particularly through the development of non-animal new
 488 approach methodologies (NAMs) (Jaylet et al., 2024; OECD, 2017). In this study, we present
 489 and analyse the first AOP-Wiki-derived network for cardiotoxicity, providing a structured
 490 overview of a diverse range of mechanisms leading to cardiac damage. The current network
 491 is not intended to be the most comprehensive collection of mechanistic understanding on
 492 cardiotoxicity mode-of-action, as it is built from linear AOPs available in AOP-Wiki. This
 493 resource is intended as a living document, capable of being iteratively updated as new AOPs

494 linking chemical exposure to cardiac outcomes are identified. Incorporating evidence from
495 optimised review methodologies (Van Ertvelde et al., 2023) and data-driven approaches for
496 KE and KER discovery (Gadaleta et al., 2024; Ortega-Vallbona et al., 2024) will
497 progressively expand its scope and improve mechanistic understanding of how chemicals
498 affect the heart.

499 Nevertheless, our analysis of the AOP-Wiki-derived network revealed an emerging
500 landscape for cardiotoxicity in the database. Most of the KEs identified (n=47; 73.4%) are
501 part of only one AOP, indicating limited interconnectivity within the current set of
502 cardiotoxicity-related pathways. Yet, the topology still exposed a small set of cross-cutting
503 KEs that organise information flow across modules. For example, “Oxidative Stress
504 (KE1392, KE1115)” consistently ranked at the top or among the highest in degree,
505 betweenness, stress, and simple-path occurrence, and also led the combined importance
506 score. Oxidative stress is a complex imbalance between reactive oxygen species (ROS)
507 production and antioxidant capacity; while transient ROS is involved in redox signalling,
508 prolonged elevation drives disease progression (Carrasco et al., 2021). Mechanistically, this
509 aligns with the well-established role of ROS imbalance as a determinant of cardiac injury
510 (Carrasco et al., 2021). This finding is also consistent with the central role of oxidative stress
511 in cardiotoxicity induced by anthracyclines like doxorubicin, idarubicin, and daunorubicin
512 (Mamoshina et al., 2021) and environmental toxicants such as heavy metals (e.g., lead,
513 cadmium, arsenic) (Ozarde et al., 2025; Pan et al., 2024). From heavy metals,
514 cardiovascular risk is induced via excessive ROS generation, overwhelming natural
515 antioxidant defences, leading to endothelial dysfunction, vascular inflammation, and
516 ultimately, hypertension and atherosclerosis (Ozarde et al., 2025; Pan et al., 2024).
517 Differently, anthracyclines trigger mitochondrial dysfunctions leading to hypoxia and
518 myocardial fibrosis, ultimately developing into heart failure (Carrasco et al., 2021). Similarly,
519 oxidative stress, along with mitochondrial dysfunction, was identified as one of the most
520 highly connected and central key events in AOP networks for hepatotoxicity (Van Ertvelde et
521 al., 2023; Verhoeven et al., 2024), neurotoxicity (Spinu et al., 2019) and nephrotoxicity
522 (Barnes et al., 2024), showcasing it as a fundamental pillar of cellular toxicity across different
523 organs.

524 Within the heart-related KEs in our network, “Decrease, Cardiac contractility (KE1532)” and
525 “Mitochondrial dysfunction (KE177, KE40)”, joined oxidative stress as a functional triad of
526 hubs. All three had high total degree and betweenness and were repeatedly visited along
527 MIE to AO simple paths. Their co-occurrence is mechanistically coherent: mitochondrial
528 impairment increases ROS and compromises ATP supply; both processes depress
529 excitation-contraction coupling and sarcomeric function, reducing contractile output
530 (Carrasco et al., 2021; Varga et al., 2015). These KEs are therefore sensitive integrators of
531 injury signals from diverse initiators (e.g., ion-channel perturbations, AhR activation, electron
532 transport chain inhibition). At the same time, they lack mode-of-action specificity, an
533 important consideration for interpreting positive signals in screening and for deciding which
534 complementary, more specific readouts to pair with them.

535 Outcome-related nodes, including “Increased Mortality (KE351, KE947, KE1929)”,
536 “Decrease, Cardiac ejection fraction (KE1533)”, “Increase, Cardiac remodelling (KE2084)”,
537 “Hypoxia (KE590)” and “Torsades de Pointes (KE1963)”, displayed low eccentricity,
538 indicating they are or they are close to terminal endpoints. Among these, “Increased
539 Mortality” further exhibited high stress centrality, confirming its central role in the network

540 where most upstream routes converge. In contrast, several initiator-proximal or extra-cardiac
541 KEs (e.g., “Inhibition, Cyclooxygenase 1 activity (KE1103)”; “Occurrence, tophi (urate)
542 deposition (KE1102)”) sat at the network periphery with higher eccentricity, consistent with
543 their role as upstream or system-level contributors rather than heart-intrinsic drivers. That is,
544 these nodes are more distant from others in the network, reflecting their role as early or
545 external triggers rather than direct cardiac effectors.

546 A notable and recurrent feature was the systemic integration of the heart, especially the
547 cardio-renal axis, illustrated in our interactive and contextual version of the network.
548 Extra-cardiac KEs such as “Occurrence, renal proximal tubular necrosis (KE1097)” and
549 “Increased, blood uric acid concentration (KE1096)” were among the most connected and
550 ranked near the top in betweenness and total degree, indicating high connectivity. These
551 patterns support a mechanistic bridge whereby renal injury and urate dysregulation amplify
552 systemic oxidative and inflammatory burden that exacerbates cardiac dysfunction (Ding et
553 al., 2022; Ozarde et al., 2025). In practice, this means a subset of cardiotoxic trajectories are
554 genuinely systemic and may be missed by single-organ assays. The cardio-renal axis
555 exemplifies a bidirectional scenario in which dysfunction in the kidney or heart triggers
556 pathophysiological feedback loops that accelerate damage in both organs. This cross-talk is
557 mediated by haemodynamic shifts, neurohormonal activation (particularly of the
558 renin-angiotensin-aldosterone system and sympathetic overactivity), and circulating
559 inflammatory and fibrotic factors, including protein-bound uremic toxins such as indoxyl
560 sulphate, which exert direct pro-hypertrophic and pro-fibrotic effects on cardiac tissue
561 (Lekawanvijit et al., 2012; Rangaswami et al., 2019). The network therefore provides a
562 rationale for multi-organ microphysiological systems (MPS) or staged testing strategies when
563 cardio-renal axes are implicated (Daley et al., 2022; OECD, 2017).

564 Edge-type composition also carries insight. While the majority of KERs were adjacent
565 (86.17%), a meaningful subset were non-adjacent (13.83%). These long-range links often
566 connect early molecular events to organ-level dysfunction and likely compress intermediate
567 biology that is either context-dependent or not yet curated in AOP-Wiki. They are useful for
568 scoping hazards and tracing plausible routes to outcomes, but they simultaneously flag the
569 most impactful knowledge gaps for future curation and quantification (Villeneuve et al.,
570 2018). The evidence overlays corroborate this: just over half of KERs carry high/strong
571 evidence, but fewer than 40% include any quantitative understanding. Notably, quantitative
572 links are sparse precisely around the hub KEs, where they would most enable quantitative
573 AOP (qAOP) development, sensitivity analyses, and extrapolation (OECD, 2017; Spinu et
574 al., 2020).

575 Together, these structural and evidential features converge on a clear message. First,
576 oxidative stress, mitochondrial dysfunction, and decreased contractility form a core,
577 recurrent axis across mechanistic routes from diverse initiators to cardiac adverse outcomes;
578 they should be prioritised for measurement and, where possible, for quantitative linkage.
579 Second, cardio-renal crosstalk is not incidental: kidney-centred KEs frequently mediate
580 routes to cardiac outcomes and warrant explicit consideration when designing evaluation
581 strategies. Third, while hub KEs are powerful integrators, they require pairing with more
582 specific, pathway-diagnostic readouts to improve mode-of-action resolution. These
583 conclusions directly inform the design principles of a mechanistically anchored, animal-free
584 cardiotoxicity testing battery, as discussed next.

586 4.1 From AOP network to an animal-free cardiotoxicity testing battery

587 A primary goal of developing this network is to inform the design of a mechanistically
588 anchored, animal-free test battery for cardiotoxicity prediction. To this end, we systematically
589 reviewed the methods section of the KE pages at AOP-Wiki and extracted the reported
590 methods to quantify and monitor individual KEs. Explicit detection methods were listed for
591 only 43.75% of unique KEs, pointing to a scattered knowledge base. The documented
592 approaches spanned *in vivo*, *in vitro*, and *in silico* methods, including biochemical assays,
593 imaging, and electrophysiological readouts. While this catalogue provides a foundational
594 starting point, it is not exhaustive and reflects the current state of user-based reporting within
595 the AOP-Wiki, which itself has limitations. A recent analysis of the AOP-Wiki showed that
596 fields describing supporting evidence are often incomplete (Jaylet et al., 2024), which likely
597 extends to the methodologies for measuring KEs.

598 Despite these gaps, the AOP network helps prioritise what to measure. Hub KEs shared
599 across multiple AOPs are efficient assay targets, but specificity is also essential for an
600 informative battery. Non-specific KEs, such as oxidative stress, mitochondrial dysfunction,
601 and cytotoxicity, are common across organ systems and chemical classes and cannot, on
602 their own, discriminate specific cardiotoxic liability (Arnesdotter et al., 2021; Barnes et al.,
603 2024; Mamoshina et al., 2021). In contrast, cardiac-specific KEs provide higher diagnostic
604 value: hERG/IKr blockade is the canonical driver of drug-induced QT prolongation and
605 torsades de pointes risk, while additional mechanisms include inhibition of cardiomyocyte
606 survival signalling (e.g., VEGF/EGF pathways) and perturbations of contractility or calcium
607 handling (Clark et al., 2022; Lester, 2021, p. 202; Mamoshina et al., 2021). Accordingly, an
608 effective test battery should follow an Integrated Approaches to Testing and Assessment
609 (IATA) logic, combining general cellular-health assays (e.g., viability, mitochondrial function)
610 with targeted tests of cardiac-specific mechanisms (e.g., multi-ion channel panels,
611 contractility, calcium cycling), to cover the relevant mechanism space (Daley et al., 2022;
612 OECD, 2017, 2020; Schaffert et al., 2023).

613 In this sense, the ALTERNATIVE project has developed an AOP-informed IATA that
614 integrates data from human-relevant *in vitro* assays, transcriptomics, and high-content
615 screening to evaluate environmental chemicals' toxicity (Schaffert, Murugadoss, et al., 2024;
616 Schaffert, Paparella, et al., 2024). This framework supports evaluating cardiotoxic liability
617 through both general and cardiac-specific endpoints, structured along mechanistic axes such
618 as contractility, electrophysiology, and cell viability. Nevertheless, unmet opportunities for
619 including other molecular strategies could still be explored, especially to detect mixture or
620 multi-target interaction outcomes, quantitative links from KEs to phenotypic dynamics, and
621 explicit sources of biological variability in predictions. Considering a broader scenario of
622 mechanism possibilities, by incorporating nuclear and membrane receptors and compound
623 metabolism pathways, among other modulators, would further enrich the current
624 understanding and help uncover novel modes of action. This holistic inclusion could capture
625 compound- and population-specific vulnerabilities, thereby advancing the refinement of
626 predictive, human-relevant cardiotoxicity testing.

627 Mechanistic compound controls (i.e., positive compound controls with well-described
628 mechanisms of action) are essential to calibrate and validate such a battery (Verhoeven et

629 al., 2025). Compounds with well-characterised modes of action allow sensitivity/specificity
630 checks and enable cross-platform comparisons (Parish et al., 2020). For instance,
631 moxifloxacin serves as a standard positive control for reproducible and multi-method
632 comparisons of QT intervals (Darpo et al., 2006); doxorubicin anchors structural
633 cardiotoxicity via mitochondrial damage and oxidative stress (Chen et al., 2023); and
634 verapamil illustrates that hERG block does not necessarily translate into proarrhythmia due
635 to compensatory calcium-current effects (Daley et al., 2022). Curated drug sets, as from
636 CiPA, further link assay outputs to established clinical outcomes and strengthen external
637 validity (Konala et al., 2025). Similarly, the FDA-labelling-based Drug-Induced Cardiotoxicity
638 rank (DICTrank) compendium (1318 drugs; severity linked to the Boxed Warning, Warnings
639 and Precautions, and Adverse Reactions sections of FDA labels) offers a clinically grounded
640 reference that shows high concordance with the Drug-Induced QT prolongation risk
641 Assessment (DIQTA) database and the CredibleMeds clinical risk classification (Qu et al.,
642 2023). The cardiotoxicity AOP network provides a mechanistic scaffold to interpret these
643 control compounds in a broader biological context. It enables the mapping of
644 compound-induced events to specific key events and pathways, clarifying the coverage of
645 relevant mechanisms across assays. This not only supports rational selection and
646 interpretation of positive controls but also the comparison and benchmarking of new test
647 systems to clinically established mechanisms.

648 Alignment with regulatory expectations is also required. In the pharmaceutical domain,
649 cardiotoxicity assessment is underpinned by ICH safety pharmacology and proarrhythmia
650 guidelines (FDA, 2005, 2021). ICH S7A defines the core safety-pharmacology battery and
651 general principles, including dedicated cardiovascular evaluations to protect trial participants
652 while minimising animal use (FDA, 2021). ICH S7B specifies a nonclinical strategy centred
653 on *in vitro* IKr (hERG) assays and *in vivo* QT studies, supported by an integrated risk
654 assessment to judge delayed ventricular repolarisation risk (FDA, 2005). Clinically, ICH E14
655 established the thorough QT paradigm and formalised links between nonclinical findings and
656 clinical proarrhythmic risk (EMA, 2022). Together, these guidances constitute a mature,
657 QT-centric framework that has reduced proarrhythmic liabilities; however, it can be
658 conservative, and recent updates recognising “double-negative” outcomes in best-practice
659 nonclinical assays signal a gradual shift toward integrated, mechanism-based assessments
660 (Lester, 2021). By contrast, current guidelines for industrial chemicals, pesticides and
661 biocides largely neglect functional cardiotoxicity, focusing instead on endpoints such as heart
662 weight and histopathology from animal studies (Schaffert et al., 2023). OECD has advanced
663 IATA and the use of AOPs to organise non-animal evidence for decision-making, including
664 guidance on IATA concepts, reporting of defined approaches and case-study programmes.
665 Acceptance and validation principles for new methods are codified in an OECD Guidance
666 Document, supporting international uptake once fitness-for-purpose is demonstrated (OECD,
667 2017). Nonetheless, the lack of quantitative key-event relationship data remains a barrier to
668 regulatory utility, underscoring the need for quantitative integration if functional cardiotoxicity
669 is to be addressed systematically and mechanistically.

670 NAMs based on human-induced pluripotent stem cell-derived cardiomyocytes (hiPSC-CMs)
671 enable high-throughput, human-relevant assessment of cardiac liabilities (Daley et al., 2022;
672 Gisone et al., 2022). Within our network, three hub KEs emerged in the heart network:
673 oxidative stress, mitochondrial dysfunction and decreased contractility, and each can be
674 measured with established assays. For decreased contractility, hiPSC-CMs provide

675 functional readouts such as beating frequency, contraction amplitude and calcium handling,
676 capturing disturbances in both electrophysiological and contractile function (Dou et al.,
677 2022). Mitochondrial dysfunction can be detected via membrane potential (e.g., using TMRE
678 fluorescent probe), oxygen consumption rate (e.g., Seahorse extracellular flux analysis) and
679 ATP production (e.g., luciferase-based assays), endpoints particularly relevant for
680 energetics-impairing compounds (e.g., anthracyclines) (Sharma et al., 2025). Oxidative
681 stress can be quantified by ROS formation, lipid peroxidation and alterations in antioxidant
682 enzyme dynamics (Murphy et al., 2022).

683 Combining these complementary readouts enables a battery that captures convergent
684 mechanisms of cardiotoxicity. This strategy moves beyond single-endpoint assays such as
685 hERG, which although sensitive, lack specificity and mechanistic breadth (Daley et al.,
686 2022). CiPA already demonstrated the value of integrating multiple ion-channel assays with
687 *in silico* modelling (Lester, 2021). Our AOP network supports extending this principle to
688 non-electrophysiological endpoints essential for detecting structural, contractile and
689 metabolic toxicities. In sum, our AOP network provides the organising principle for designing
690 an animal-free test battery and the curated catalogue of KE measurement methods identifies
691 immediate assay candidates and evidence gaps.

692

693 4.2 Challenges, opportunities and future perspectives

694 A significant challenge encountered during this work was the lack of standardisation in the
695 AOP-Wiki, a scenario also identified in other mapping studies (Jaylet et al., 2024). Many KEs
696 describing the same biological process were titled differently, requiring manual
697 harmonisation to build a coherent network. For instance, events with overlapping biological
698 scope were recorded under multiple names and with different levels of detail, which
699 fragments knowledge and complicates automated network generation. These redundancies
700 have been explicitly noted for ROS-related KEs, where multiple nuanced entries exist
701 despite referring to similar processes, prompting the launch of the “Mystery of ROS” initiative
702 to create harmonised consensus KEs (Tanabe et al., 2022, 2023). Such efforts highlight the
703 broader need for ontology-based alignment of KE terminology, ensuring consistency in
704 descriptors like directionality, biological objects, and processes to make entries
705 machine-readable and interoperable. This demand has been echoed by the Society for the
706 Advancement of AOPs Knowledgebase Interest Group (SKIG), which has prioritised
707 ontology-driven harmonisation, systematic curation, and development of umbrella KEs as
708 central steps towards AOP-Wiki 3.0 (Wittwehr et al., 2025). In parallel, the recently launched
709 SCAHT AOP_HUB provides a practical forum for training, knowledge exchange, and
710 discussion of recurring challenges in AOP development, with a strong focus on engaging
711 early-career researchers (Coerek et al., 2025). Together, these initiatives demonstrate that
712 the community is actively addressing the standardisation bottleneck and moving towards a
713 more interoperable and predictive AOP knowledge base.

714 Furthermore, the current AOP framework in the AOP-Wiki insufficiently captures feedback
715 loops and compensatory mechanisms, which are essential to understand the dose- and
716 time-dependent nature of cardiotoxicity (Georgiadis et al., 2022; Mamoshina et al., 2021).
717 Linear AOPs, by design, tend to oversimplify complex biological responses, whereas AOP
718 networks offer a more realistic systems-level representation of toxicity by accounting for
719 converging and diverging pathways (Sewell et al., 2018). Our network begins to address this

720 by linking multiple MIEs to shared KEs, but a more explicit integration of dynamic motifs -
721 such as feedback and feedforward regulation, as highlighted in AOP network development
722 frameworks (Knapen et al., 2018; Villeneuve et al., 2018) - would significantly enhance its
723 predictive power. In this direction, the Disease Maps community (<https://disease-maps.io/>)
724 has demonstrated that mechanistic, highly detailed molecular maps enable systematic
725 integration of multi-omics data and contextual interpretation of dynamic processes, providing
726 a promising blueprint for advancing AOPs beyond static representations and tools for
727 benchmarking existing networks (Ladeira et al., 2025; Mazein et al., 2018; Staumont et al.,
728 2025). Moving from the mostly high-level representation of biological activities in the
729 AOP-Wiki towards more detailed molecular maps would improve interpretability of
730 experimental outcomes and mechanistic grounding. This does not require enforcing
731 excessive pathway granularity but can be achieved through complementary strategies such
732 as ontology mapping, pathway enrichment analysis, and the application of computational
733 approaches for quantitative AOP modelling (Jaylet et al., 2024; Knapen et al., 2018).

734 Importantly, such advances depend on making AOP knowledge not only interoperable but
735 also machine-actionable. Recent work has stressed that adherence to the FAIR principles
736 (ensuring that AOPs are Findable, Accessible, Interoperable, and Reusable) is essential to
737 increase their visibility, credibility, and uptake in regulatory decision-making (Wittwehr et al.,
738 2023). FAIRification enables automation, provenance tracking, and semantic alignment,
739 addressing current issues of network fragmentation and enhancing trust in AOP-derived
740 models. In this context, detailed molecular mapping does not merely increase complexity but
741 creates opportunities for advanced visualisation, data integration, and predictive modelling.
742 A recent example is the explorable model of cytokine release syndrome developed by
743 Mazein et al. (2025), which integrates multiple AOPs induced by immunomodulatory
744 therapies into a molecular-level systems biology map. By combining diagrammatic KE
745 representations with machine-readable formats (e.g., SBML, SBGN, stable identifiers), this
746 resource ensures reproducibility and interoperability while enabling hypothesis generation,
747 biomarker discovery, and mechanistic modelling. Collectively, these directions underscore
748 the need for cross-disciplinary integration of systems biology and toxicology to make
749 AOP-based models more dynamic, predictive, FAIR and regulatory-relevant.

750 A major opportunity ahead is the transition from qualitative AOP networks to qAOP models.
751 By parameterising key event relationships with dose-response and time-course data, qAOPs
752 can predict the magnitude or likelihood of an adverse outcome from defined perturbations at
753 the molecular level (Conolly et al., 2017; Spinu et al., 2020). Such dynamic models can be
754 implemented through diverse approaches, from Bayesian and regression-based methods to
755 mechanistic ODE frameworks or logic-based modelling, chosen according to data availability
756 and context-of-use (Paini et al., 2022; Perkins et al., 2019). When coupled with
757 physiologically based pharmacokinetic or quantitative systems pharmacology models, they
758 enable quantitative *in vitro*-to-*in vivo* extrapolation, translating cell-based assay data into
759 exposure thresholds relevant for humans (Proença et al., 2021; Sang et al., 2024). This
760 integrative direction has already demonstrated predictive capacity for drug-induced
761 cardiotoxicity (Sang et al., 2024), underscoring its potential for translational applications.
762

763 4.3 Concluding remarks

764 This study provides the first integrated AOP network for cardiotoxicity, transforming the
765 current knowledge in the OECD AOP-Wiki into a coherent map of cardiac hazard. The
766 analysis identified oxidative stress, mitochondrial dysfunction, and decreased contractility as
767 central, highly connected key events that serve as the primary convergence points of diverse
768 chemical stressors. Importantly, the network highlights the systemic nature of cardiotoxicity,
769 with the cardio-renal axis acting as a mechanistic bridge that is not captured by
770 channel-centric assays. These findings provide a strong mechanistic foundation for
771 designing an animal-free and human-relevant test battery using a diverse collection of
772 methods, including multi-organ models to address complex mechanisms. While the sparsity
773 in the source data highlights the need for greater standardisation and curation within the
774 AOP community, our work demonstrates the power of the AOP network framework to
775 synthesise complex toxicological information and serves as a guiding resource for IATA
776 design and the prioritization of animal-free testing strategies. Our KE-assay catalogue and
777 the FAIR-aligned interactive and contextual map provides the community with a living
778 scaffold that can be iteratively refined with emerging evidence. Future work should evolve
779 the networks into qAOPs integrated with detailed systems-biology maps to create dynamic
780 tools for assessing cardiovascular hazard and risk and ensuring the safety of both new drugs
781 and environmental chemicals.

782

783 Funding

784 This work received funding from the European Research Council under the European
785 Union's Horizon Europe Framework Program / ERC grant agreement No 101088919
786 (INSTant CARMA).

787

788 Declaration of competing interests

789 The authors declare they have no competing interests.

790

791 Declaration of Generative AI and AI-assisted technologies in the 792 writing process

793 During the preparation of this work, the authors used Gemini 3 (Google) in order to assist
794 with language editing. After using this tool/service, the authors reviewed and edited the
795 content as needed and take full responsibility for the content of the publication.

796

797 Consent for publication

798 All authors agree to the publication of this study.

799

800 CRediT author statement

801 **Luiz Ladeira:** Conceptualization, Methodology, Software, Investigation, Data Curation,

802 Project administration, Writing - Original Draft, Visualization, Writing - Review & Editing.
803 **Devon Barnes:** Methodology, Investigation, Writing - Review & Editing. **Rosalinde**
804 **Masereeuw:** Methodology, Investigation, Writing - Review & Editing. **Liesbet Geris:**
805 Conceptualization, Methodology, Resources, Writing - Review & Editing, Supervision, Project
806 administration, Funding acquisition. **Bernard Staumont:** Conceptualization, Methodology,
807 Resources, Writing - Review & Editing, Supervision.
808

809 Acknowledgements

810 The authors thank Hesam Korki and Valentin Groues for their support in developing the
811 MINERVA plugin. We also thank Professor Dr. Luigi Margiotta-Casaluci for granting
812 permission to use data from AOP 261, which is under an “all rights reserved” licence. We
813 thank the ONTOX project for hosting the interactive map at the MINERVA platform. Online
814 browsing of the interactive model is provided by the MINERVA team
815 (<https://minerva.pages.uni.lu/doc/>) at the Bioinformatics Core of the Luxembourg Centre for
816 Systems Biomedicine, within the ELIXIR-LU framework (<https://elixir-luxembourg.org>). This
817 work was supported by ELIXIR Luxembourg.
818

819 Data availability

820 The datasets are available on GitHub
821 (https://github.com/luiz-ladeira/cardiotox_aop_minerva_plugin) and on the MINERVA
822 platform (https://ontox.elixir-luxembourg.org/minerva/index.html?id=cardiotox_aop), under
823 the Creative Commons Attribution 4.0 International (CC BY 4.0) License
824 (<https://creativecommons.org/licenses/by/4.0/>).
825

826 List of abbreviations

827 AchE: Acetylcholinesterase
828 AF: Activity Flow
829 AhR: Aryl hydrocarbon receptor
830 AO: Adverse Outcome
831 AOP: Adverse Outcome Pathway
832 CiPA: Comprehensive *in vitro* Proarrhythmia Assay
833 COX-2: Cyclooxygenase-2
834 COX1: Cyclooxygenase 1
835 DICTrank: Drug-Induced Cardiotoxicity rank
836 DIQTA: Drug-Induced QT prolongation risk Assessment
837 EGF: Epidermal Growth Factor
838 FAIR: Findable, Accessible, Interoperable, and Reusable
839 FDA: Food and Drug Administration
840 hERG: Human Ether-à-go-go Related Gene
841 hiPSC-CMs: Human-induced pluripotent stem cell-derived cardiomyocytes
842 IATA: Integrated Approaches to Testing and Assessment
843 ICH: International Conference on Harmonization
844 IKr: Rapid component of the delayed rectifier potassium current

845 KE: Key Event
846 KERs: Key Event Relationships
847 LV: Left Ventricle
848 MIE: Molecular Initiating Event
849 MINERVA: Molecular Interaction NEtwork VisuAlization (platform)
850 MPS: Microphysiological systems
851 nAChR: Nicotinic Acetylcholine Receptor
852 NAMs: New Approach Methodologies
853 OAT1: Organic anion transporter 1
854 OECD: Organisation for Economic Co-operation and Development
855 qAOP: Quantitative Adverse Outcome Pathway
856 QT/QTc: QT interval / corrected QT interval
857 ROS: Reactive Oxygen Species
858 SBGN: Systems Biology Graphical Notation
859 SBML: Systems Biology Markup Language
860 SKIG: Society for the Advancement of AOPs Knowledgebase Interest Group
861 TMRE - Tetramethylrhodamine, ethyl ester
862 VEGF: Vascular Endothelial Growth Factor
863 WPHA: Working Party on Hazard Assessment
864 WNT: Working Group of the National Coordinators of the Test Guidelines Programme
865

866 References

867 Amani Farhat & Sean W. Kennedy. (2019). *Adverse Outcome Pathway on Aryl hydrogen*
868 *receptor activation leading to early life stage mortality, via reduced VEGF* (OECD
869 Series on Adverse Outcome Pathways No. 16; OECD Series on Adverse Outcome
870 Pathways, Vol. 16). OECD. <https://doi.org/10.1787/063e1bf4-en>

871 Ankley, G. T., Bennett, R. S., Erickson, R. J., Hoff, D. J., Hornung, M. W., Johnson, R. D.,
872 Mount, D. R., Nichols, J. W., Russom, C. L., Schmieder, P. K., Serrano, J. A., Tietge,
873 J. E., & Villeneuve, D. L. (2009). Adverse outcome pathways: A conceptual
874 framework to support ecotoxicology research and risk assessment. *Environmental*
875 *Toxicology and Chemistry*, 29(3), 730–741. <https://doi.org/10.1002/etc.34>

876 Arnesdotter, E., Spinu, N., Firman, J., Ebbrell, D., Cronin, M. T. D., Vanhaecke, T., & Vinken,
877 M. (2021). Derivation, characterisation and analysis of an adverse outcome pathway
878 network for human hepatotoxicity. *Toxicology*, 459, 152856.
879 <https://doi.org/10.1016/j.tox.2021.152856>

880 Bajard, L., Adamovsky, O., Audouze, K., Baken, K., Barouki, R., Beltman, J. B., Beronius, A.,
881 Bonefeld-Jørgensen, E. C., Cano-Sancho, G., De Baat, M. L., Di Tillio, F., Fernández,
882 M. F., FitzGerald, R. E., Gundacker, C., Hernández, A. F., Hilscherova, K.,
883 Karakitsios, S., Kuchovska, E., Long, M., ... Blaha, L. (2023). Application of AOPs to
884 assist regulatory assessment of chemical risks – Case studies, needs and
885 recommendations. *Environmental Research*, 217, 114650.
886 <https://doi.org/10.1016/j.envres.2022.114650>

887 Barnes, D. A., Firman, J. W., Belfield, S. J., Cronin, M. T. D., Vinken, M., Janssen, M. J., &
888 Masereeuw, R. (2024). Development of an adverse outcome pathway network for
889 nephrotoxicity. *Archives of Toxicology*, 98(3), 929–942.
890 <https://doi.org/10.1007/s00204-023-03637-7>

891 Carrasco, R., Castillo, R. L., Gormaz, J. G., Carrillo, M., & Thavendiranathan, P. (2021). Role
892 of Oxidative Stress in the Mechanisms of Anthracycline-Induced Cardiotoxicity:
893 Effects of Preventive Strategies. *Oxidative Medicine and Cellular Longevity*, 2021(1),
894 8863789. <https://doi.org/10.1155/2021/8863789>

895 Chen, R., Niu, M., Hu, X., & He, Y. (2023). Targeting mitochondrial dynamics proteins for the
896 treatment of doxorubicin-induced cardiotoxicity. *Frontiers in Molecular Biosciences*,
897 10, 1241225. <https://doi.org/10.3389/fmolb.2023.1241225>

898 Clark, A. P., Wei, S., Kalola, D., Krogh-Madsen, T., & Christini, D. J. (2022). An in silico–in
899 vitro pipeline for drug cardiotoxicity screening identifies ionic pro-arrhythmia
900 mechanisms. *British Journal of Pharmacology*, 179(20), 4829–4843.
901 <https://doi.org/10.1111/bph.15915>

902 Coerek, E., Kuchovska, E., Gerner, L., Nilma, L., Villeneuve, D., & Fritsche, E. (2025). The
903 SCAHT Adverse Outcome Pathway (AOP)_HUB: A hands-on platform for information

904 exchange, sharing, and developing AOPs. *ALTEX*, 42(2).
905 <https://doi.org/10.14573/altex.2502051>

906 Conolly, R. B., Ankley, G. T., Cheng, W., Mayo, M. L., Miller, D. H., Perkins, E. J., Villeneuve,
907 D. L., & Watanabe, K. H. (2017). Quantitative Adverse Outcome Pathways and Their
908 Application to Predictive Toxicology. *Environmental Science & Technology*, 51(8),
909 4661–4672. <https://doi.org/10.1021/acs.est.6b06230>

910 Daley, M., Mende, U., Choi, B.-R., McMullen, P. D., & Coulombe, K. L. K. (2022). Beyond
911 pharmaceuticals: Fit-for-purpose new approach methodologies for environmental
912 cardiotoxicity testing. *ALTEX*. <https://doi.org/10.14573/altex.2109131>

913 Darpo, B., Nebout, T., & Sager, P. T. (2006). Clinical Evaluation of QT/QTc Prolongation and
914 Proarrhythmic Potential for Nonantiarrhythmic Drugs: The International Conference
915 on Harmonization of Technical Requirements for Registration of Pharmaceuticals for
916 Human Use E14 Guideline. *The Journal of Clinical Pharmacology*, 46(5), 498–507.
917 <https://doi.org/10.1177/0091270006286436>

918 Ding, R., Ren, X., Sun, Q., Sun, Z., & Duan, J. (2022). An integral perspective of canonical
919 cigarette and e-cigarette-related cardiovascular toxicity based on the adverse
920 outcome pathway framework. *Journal of Advanced Research*, S209012322200193X.
921 <https://doi.org/10.1016/j.jare.2022.08.012>

922 Dou, W., Malhi, M., Zhao, Q., Wang, L., Huang, Z., Law, J., Liu, N., Simmons, C. A., Maynes,
923 J. T., & Sun, Y. (2022). Microengineered platforms for characterizing the contractile
924 function of in vitro cardiac models. *Microsystems & Nanoengineering*, 8(1), 26.
925 <https://doi.org/10.1038/s41378-021-00344-0>

926 EMA. (2022). *ICH guideline E14/S7B: clinical and nonclinical evaluation of QT/QTc interval*
927 *prolongation and proarrhythmic potential—Questions and answers—Scientific*
928 *guideline*.

929 FDA. (2005). *S7B Nonclinical Evaluation of the Potential for Delayed Ventricular*
930 *Repolarization (QT Interval Prolongation) by Human Pharmaceuticals.*

931 FDA. (2021). *S7A Safety Pharmacology Studies for Human Pharmaceuticals.*

932 Funahashi, A., Matsuoka, Y., Jouraku, A., Morohashi, M., Kikuchi, N., & Kitano, H. (2008).
933 CellDesigner 3.5: A Versatile Modeling Tool for Biochemical Networks. *Proceedings*
934 *of the IEEE*, 96(8), 1254–1265. <https://doi.org/10.1109/JPROC.2008.925458>

935 Gadaleta, D., Garcia De Lomana, M., Serrano-Candelas, E., Ortega-Vallbona, R., Gozalbes,
936 R., Roncaglioni, A., & Benfenati, E. (2024). Quantitative structure–activity
937 relationships of chemical bioactivity toward proteins associated with molecular
938 initiating events of organ-specific toxicity. *Journal of Cheminformatics*, 16(1), 122.
939 <https://doi.org/10.1186/s13321-024-00917-x>

940 Gawron, P., Hoksza, D., Piñero, J., Peña-Chilet, M., Esteban-Medina, M., Fernandez-Rueda,
941 J. L., Colonna, V., Smula, E., Heirendt, L., Ancien, F., Groues, V., Satagopam, V. P.,
942 Schneider, R., Dopazo, J., Furlong, L. I., & Ostaszewski, M. (2023). Visualization of
943 automatically combined disease maps and pathway diagrams for rare diseases.
944 *Frontiers in Bioinformatics*, 3, 1101505. <https://doi.org/10.3389/fbinf.2023.1101505>

945 Georgiadis, N., Tsarouhas, K., Dorne, J.-L. C. M., Kass, G. E. N., Laspa, P., Toutouzas, K.,
946 Koulaouzidou, E. A., Kouretas, D., & Tsitsimpikou, C. (2022). Cardiotoxicity of
947 Chemical Substances: An Emerging Hazard Class. *Journal of Cardiovascular*
948 *Development and Disease*, 9(7), 226. <https://doi.org/10.3390/jcdd9070226>

949 Gisone, I., Cecchettini, A., Ceccherini, E., Persiani, E., Morales, M. A., & Vozi, F. (2022).
950 Cardiac tissue engineering: Multiple approaches and potential applications. *Frontiers*
951 *in Bioengineering and Biotechnology*, 10, 980393.
952 <https://doi.org/10.3389/fbioe.2022.980393>

953 Global Burden of Cardiovascular Diseases and Risks 2023 Collaborators. (2025). Global,
954 Regional, and National Burden of Cardiovascular Diseases and Risk Factors in 204
955 Countries and Territories, 1990-2023. *JACC*, S0735109725074285.
956 <https://doi.org/10.1016/j.jacc.2025.08.015>

957 Hoksza, D., Gawron, P., Ostaszewski, M., Hasenauer, J., & Schneider, R. (2020). Closing
958 the gap between formats for storing layout information in systems biology. *Briefings*
959 *in Bioinformatics*, 21(4), 1249–1260. <https://doi.org/10.1093/bib/bbz067>

960 Hoksza, D., Gawron, P., Ostaszewski, M., Smula, E., & Schneider, R. (2019). MINERVA API
961 and plugins: Opening molecular network analysis and visualization to the community.
962 *Bioinformatics*, 35(21), 4496–4498. <https://doi.org/10.1093/bioinformatics/btz286>

963 Jaylet, T., Coustillet, T., Smith, N. M., Viviani, B., Lindeman, B., Vergauwen, L., Myhre, O.,
964 Yarar, N., Gostner, J. M., Monfort-Lanzas, P., Jornod, F., Holbech, H., Coumoul, X.,
965 Sarigiannis, D. A., Antczak, P., Bal-Price, A., Fritsche, E., Kuchovska, E., Stratidakis,
966 A. K., ... Audouze, K. (2024). Comprehensive mapping of the AOP-Wiki database:
967 Identifying biological and disease gaps. *Frontiers in Toxicology*, 6, 1285768.
968 <https://doi.org/10.3389/ftox.2024.1285768>

969 Jon Doering, Markus Hecker, & Xiaowei Zhang. (2019). *Adverse Outcome Pathway on aryl*
970 *hydrocarbon receptor activation leading to early life stage mortality, via increased*
971 *COX-2* (OECD Series on Adverse Outcome Pathways No. 12; OECD Series on
972 *Adverse Outcome Pathways, Vol. 12*). OECD. <https://doi.org/10.1787/bd46b538-en>

973 Knapen, D., Angrish, M. M., Fortin, M. C., Katsiadaki, I., Leonard, M., Margiotta-Casaluci, L.,
974 Munn, S., O'Brien, J. M., Pollesch, N., Smith, L. C., Zhang, X., & Villeneuve, D. L.
975 (2018). Adverse outcome pathway networks I: Development and applications.
976 *Environmental Toxicology and Chemistry*, 37(6), 1723–1733.
977 <https://doi.org/10.1002/etc.4125>

- 978 Konala, V. B. R., Kuhikar, R., More, S., Gossmann, M., Lickiss, B., Linder, P., Sarkar, J.,
979 Bhanushali, P., & Khanna, A. (2025). CiPA-qualified human iPSC-derived
980 cardiomyocytes: A new frontier in toxicity testing by evaluating drug-induced
981 arrhythmias. *Toxicology in Vitro*, *108*, 106100.
982 <https://doi.org/10.1016/j.tiv.2025.106100>
- 983 Ladeira, L., Verhoeven, A., Van Ertvelde, J., Jiang, J., Gamba, A., Sanz-Serrano, J.,
984 Vanhaecke, T., Heusinkveld, H. J., Jover, R., Vinken, M., Geris, L., & Staumont, B.
985 (2025). Unlocking liver physiology: Comprehensive pathway maps for mechanistic
986 understanding. *Frontiers in Toxicology*, *7*, 1619651.
987 <https://doi.org/10.3389/ftox.2025.1619651>
- 988 Lekawanvijit, S., Kompa, A. R., Wang, B. H., Kelly, D. J., & Krum, H. (2012). Cardiorenal
989 Syndrome: The Emerging Role of Protein-Bound Uremic Toxins. *Circulation*
990 *Research*, *111*(11), 1470–1483. <https://doi.org/10.1161/CIRCRESAHA.112.278457>
- 991 Lester, R. M. (2021). Update on ICH E14/S7B Cardiac Safety Regulations: The Expanded
992 Role of Preclinical Assays and the “Double-Negative” Scenario. *Clinical*
993 *Pharmacology in Drug Development*, *10*(9), 964–973.
994 <https://doi.org/10.1002/cpdd.1003>
- 995 Mamoshina, P., Rodriguez, B., & Bueno-Orovio, A. (2021). Toward a broader view of
996 mechanisms of drug cardiotoxicity. *Cell Reports. Medicine*, *2*(3), 100216.
997 <https://doi.org/10.1016/j.xcrm.2021.100216>
- 998 Mazein, A., Lopata, O., Reiche, K., Sewald, K., Alb, M., Sakellariou, C., Gogesch, P.,
999 Morgan, H., Neuhaus, V., Pham, N.-N., Sommer, C., Perkins, E., Fogal, B., Shoaib,
1000 M., Schneider, R., Satagopam, V., & Ostaszewski, M. (2025). An explorable model of
1001 an adverse outcome pathway of cytokine release syndrome related to the
1002 administration of immunomodulatory biotherapeutics and cellular therapies. *Frontiers*
1003 *in Immunology*, *16*, 1601670. <https://doi.org/10.3389/fimmu.2025.1601670>

1004 Mazein, A., Ostaszewski, M., Kuperstein, I., Watterson, S., Le Novère, N., Lefaudeux, D., De
1005 Meulder, B., Pellet, J., Balaur, I., Saqi, M., Nogueira, M. M., He, F., Parton, A.,
1006 Lemonnier, N., Gawron, P., Gebel, S., Hainaut, P., Ollert, M., Dogrusoz, U., ...
1007 Auffray, C. (2018). Systems medicine disease maps: Community-driven
1008 comprehensive representation of disease mechanisms. *Npj Systems Biology and*
1009 *Applications*, 4(1), 21. <https://doi.org/10.1038/s41540-018-0059-y>

1010 Mi, H., Schreiber, F., Moodie, S., Czauderna, T., Demir, E., Haw, R., Luna, A., Le Novere, N.,
1011 Sorokin, A., & Villegier, A. (2015). *Systems Biology Graphical Notation: Activity Flow*
1012 *language Level 1 Version 1.2*. <https://doi.org/10.2390/BIECOLL-JIB-2015-265>

1013 Mortensen, H. M., Gromelski, M., Hench, G., Martens, M., Wittwehr, C., Kumar, S., Kumar,
1014 V., Audouze, K., Virvilis, V., Nymark, P., Angrish, M., Lynch, I., Edwards, S.,
1015 Magagna, B., & Wojewodzic, M. W. (2025). The FAIR AOP roadmap for 2025:
1016 Advancing findability, accessibility, interoperability, and re-usability of adverse
1017 outcome pathways. *Computational Toxicology*, 35, 100368.
1018 <https://doi.org/10.1016/j.comtox.2025.100368>

1019 Mortensen, H. M., Martens, M., Senn, J., Levey, T., Evelo, C. T., Willighagen, E. L., & Exner,
1020 T. (2022). The AOP-DB RDF: Applying FAIR Principles to the Semantic Integration of
1021 AOP Data Using the Research Description Framework. *Frontiers in Toxicology*, 4,
1022 803983. <https://doi.org/10.3389/ftox.2022.803983>

1023 Murphy, M. P., Bayir, H., Belousov, V., Chang, C. J., Davies, K. J. A., Davies, M. J., Dick, T.
1024 P., Finkel, T., Forman, H. J., Janssen-Heininger, Y., Gems, D., Kagan, V. E.,
1025 Kalyanaraman, B., Larsson, N.-G., Milne, G. L., Nyström, T., Poulsen, H. E., Radi, R.,
1026 Van Remmen, H., ... Halliwell, B. (2022). Guidelines for measuring reactive oxygen
1027 species and oxidative damage in cells and in vivo. *Nature Metabolism*, 4(6),
1028 651–662. <https://doi.org/10.1038/s42255-022-00591-z>

- 1029 Novère, N. L., Hucka, M., Mi, H., Moodie, S., Schreiber, F., Sorokin, A., Demir, E., Wegner,
1030 K., Aladjem, M. I., Wimalaratne, S. M., Bergman, F. T., Gauges, R., Ghazal, P.,
1031 Kawaji, H., Li, L., Matsuoka, Y., Villéger, A., Boyd, S. E., Calzone, L., ... Kitano, H.
1032 (2009). The Systems Biology Graphical Notation. *Nature Biotechnology*, 27(8),
1033 735–741. <https://doi.org/10.1038/nbt.1558>
- 1034 OECD. (2017). *Guidance Document for the Use of Adverse Outcome Pathways in*
1035 *Developing Integrated Approaches to Testing and Assessment (IATA)*. OECD.
1036 <https://doi.org/10.1787/44bb06c1-en>
- 1037 OECD. (2018). *Users' Handbook supplement to the Guidance Document for developing and*
1038 *assessing Adverse Outcome Pathways* (OECD Series on Adverse Outcome
1039 Pathways No. 1; OECD Series on Adverse Outcome Pathways, Vol. 1).
1040 <https://doi.org/10.1787/5jlv1m9d1g32-en>
- 1041 OECD. (2020). *Overview of Concepts and Available Guidance related to Integrated*
1042 *Approaches to Testing and Assessment (IATA)*. OECD.
1043 <https://doi.org/10.1787/cd920ca4-en>
- 1044 OECD. (2025). *The State of Cardiovascular Health in the European Union*. OECD
1045 Publishing. <https://doi.org/10.1787/ea7a15f4-en>
- 1046 Ortega-Vallbona, R., Palomino-Schätzlein, M., Tolosa, L., Benfenati, E., Ecker, G. F.,
1047 Gozalbes, R., & Serrano-Candelas, E. (2024). Computational Strategies for
1048 Assessing Adverse Outcome Pathways: Hepatic Steatosis as a Case Study.
1049 *International Journal of Molecular Sciences*, 25(20), 11154.
1050 <https://doi.org/10.3390/ijms252011154>
- 1051 Ozarde, Y., Purandare, D., Deshmukh, S., & Gadhave, R. (2025). Heavy metals and
1052 cardiovascular health: Uncovering links and health challenges. *Journal of Trace*

- 1053 *Elements in Medicine and Biology*, 89, 127648.
1054 <https://doi.org/10.1016/j.jtemb.2025.127648>
- 1055 Paini, A., Campia, I., Cronin, M. T. D., Asturiol, D., Ceriani, L., Exner, T. E., Gao, W., Gomes,
1056 C., Kruisselbrink, J., Martens, M., Meek, M. E. B., Pamies, D., Pletz, J., Scholz, S.,
1057 Schüttler, A., Spînu, N., Villeneuve, D. L., Wittwehr, C., Worth, A., & Luijten, M.
1058 (2022). Towards a qAOP framework for predictive toxicology—Linking data to
1059 decisions. *Computational Toxicology*, 21, 100195.
1060 <https://doi.org/10.1016/j.comtox.2021.100195>
- 1061 Pan, Z., Gong, T., & Liang, P. (2024). Heavy Metal Exposure and Cardiovascular Disease.
1062 *Circulation Research*, 134(9), 1160–1178.
1063 <https://doi.org/10.1161/CIRCRESAHA.123.323617>
- 1064 Parish, S. T., Aschner, M., Casey, W., Corvaro, M., Embry, M. R., Fitzpatrick, S., Kidd, D.,
1065 Kleinstreuer, N. C., Lima, B. S., Settivari, R. S., Wolf, D. C., Yamazaki, D., & Boobis,
1066 A. (2020). An evaluation framework for new approach methodologies (NAMs) for
1067 human health safety assessment. *Regulatory Toxicology and Pharmacology*, 112,
1068 104592. <https://doi.org/10.1016/j.yrtph.2020.104592>
- 1069 Perkins, E. J., Ashauer, R., Burgoon, L., Conolly, R., Landesmann, B., Mackay, C., Murphy,
1070 C. A., Pollesch, N., Wheeler, J. R., Zupanic, A., & Scholz, S. (2019). Building and
1071 Applying Quantitative Adverse Outcome Pathway Models for Chemical Hazard and
1072 Risk Assessment. *Environmental Toxicology and Chemistry*, 38(9), 1850–1865.
1073 <https://doi.org/10.1002/etc.4505>
- 1074 Proença, S., Escher, B. I., Fischer, F. C., Fisher, C., Grégoire, S., Hewitt, N. J., Nicol, B.,
1075 Paini, A., & Kramer, N. I. (2021). Effective exposure of chemicals in in vitro cell
1076 systems: A review of chemical distribution models. *Toxicology in Vitro*, 73, 105133.
1077 <https://doi.org/10.1016/j.tiv.2021.105133>

- 1078 Qu, Y., Li, T., Liu, Z., Li, D., & Tong, W. (2023). DICTrank: The largest reference list of 1318
1079 human drugs ranked by risk of drug-induced cardiotoxicity using FDA labeling. *Drug*
1080 *Discovery Today*, 28(11), 103770. <https://doi.org/10.1016/j.drudis.2023.103770>
- 1081 Rangaswami, J., Bhalla, V., Blair, J. E. A., Chang, T. I., Costa, S., Lentine, K. L., Lerma, E.
1082 V., Mezue, K., Molitch, M., Mullens, W., Ronco, C., Tang, W. H. W., McCullough, P.
1083 A., & On behalf of the American Heart Association Council on the Kidney in
1084 Cardiovascular Disease and Council on Clinical Cardiology. (2019). Cardiorenal
1085 Syndrome: Classification, Pathophysiology, Diagnosis, and Treatment Strategies: A
1086 Scientific Statement From the American Heart Association. *Circulation*, 139(16).
1087 <https://doi.org/10.1161/CIR.0000000000000664>
- 1088 Russom, C. L., LaLone, C. A., Villeneuve, D. L., & Ankley, G. T. (2014). Development of an
1089 adverse outcome pathway for acetylcholinesterase inhibition leading to acute
1090 mortality. *Environmental Toxicology and Chemistry*, 33(10), 2157–2169.
1091 <https://doi.org/10.1002/etc.2662>
- 1092 Sang, L., Zhou, Z., Luo, S., Zhang, Y., Qian, H., Zhou, Y., He, H., & Hao, K. (2024). An In
1093 Silico Platform to Predict Cardiotoxicity Risk of Anti-tumor Drug Combination with
1094 hiPSC-CMs Based In Vitro Study. *Pharmaceutical Research*, 41(2), 247–262.
1095 <https://doi.org/10.1007/s11095-023-03644-4>
- 1096 Scardoni, G., Tosadori, G., Pratap, S., Spoto, F., & Laudanna, C. (2015). Finding the shortest
1097 path with PesCa: A tool for network reconstruction. *F1000Research*, 4, 484.
1098 <https://doi.org/10.12688/f1000research.6769.2>
- 1099 Schaffert, A., Murugadoss, S., Mertens, B., & Paparella, M. (2023). Cardiotoxicity of
1100 chemicals: Current regulatory guidelines, knowledge gaps, and needs. *ALTEX*, 40(2),
1101 337–340. <https://doi.org/10.14573/altex.2301121>

- 1102 Schaffert, A., Murugadoss, S., Paparella, M., & Mertens, B. (2024). *ALTERNATIVE*
1103 *Deliverable D2.4 General structure of IATA for cardiotoxicity* [Deliverable].
1104 <https://doi.org/10.5281/zenodo.11109364>
- 1105 Schaffert, A., Paparella, M., & Mertens, B. (2024). *ALTERNATIVE Deliverable D2.5*
1106 *Executive summary of the ALTERNATIVE project results, including questions for*
1107 *European Regulators* [Deliverable]. <https://doi.org/10.5281/zenodo.11401190>
- 1108 Sewell, F., Gellatly, N., Beaumont, M., Burden, N., Currie, R., De Haan, L., Hutchinson, T. H.,
1109 Jacobs, M., Mahony, C., Malcomber, I., Mehta, J., Whale, G., & Kimber, I. (2018).
1110 The future trajectory of adverse outcome pathways: A commentary. *Archives of*
1111 *Toxicology*, *92*(4), 1657–1661. <https://doi.org/10.1007/s00204-018-2183-2>
- 1112 Shankar, P., & Villeneuve, D. L. (2023). AOP Report: Aryl Hydrocarbon Receptor Activation
1113 Leads to Early–Life Stage Mortality via Sox9 Repression-Induced Craniofacial and
1114 Cardiac Malformations. *Environmental Toxicology and Chemistry*, *42*(10),
1115 2063–2077. <https://doi.org/10.1002/etc.5699>
- 1116 Shannon, P., Markiel, A., Ozier, O., Baliga, N. S., Wang, J. T., Ramage, D., Amin, N.,
1117 Schwikowski, B., & Ideker, T. (2003). Cytoscape: A Software Environment for
1118 Integrated Models of Biomolecular Interaction Networks. *Genome Research*, *13*(11),
1119 2498–2504. <https://doi.org/10.1101/gr.1239303>
- 1120 Sharma, E., Fotooh Abadi, L., Kombe Kombe, J. A., Kandala, M., Parker, J., Winicki, N., &
1121 Kelesidis, T. (2025). Overview of methods that determine mitochondrial function in
1122 human disease. *Metabolism*, *170*, 156300.
1123 <https://doi.org/10.1016/j.metabol.2025.156300>
- 1124 Spinu, N., Bal-Price, A., Cronin, M. T. D., Enoch, S. J., Madden, J. C., & Worth, A. P. (2019).
1125 Development and analysis of an adverse outcome pathway network for human

- 1126 neurotoxicity. *Archives of Toxicology*, 93(10), 2759–2772.
1127 <https://doi.org/10.1007/s00204-019-02551-1>
- 1128 Spinu, N., Cronin, M. T. D., Enoch, S. J., Madden, J. C., & Worth, A. P. (2020). Quantitative
1129 adverse outcome pathway (qAOP) models for toxicity prediction. *Archives of*
1130 *Toxicology*, 94(5), 1497–1510. <https://doi.org/10.1007/s00204-020-02774-7>
- 1131 Staumont, B., Ladeira, L., Gamba, A., Heusinkveld, H. J., Piersma, A., Masereeuw, R.,
1132 Vanhaecke, T., Teunis, M., Luechtefeld, T. H., Hartung, T., Jover, R., Vinken, M., &
1133 Geris, L. (2025). Mapping Physiology: A Systems Biology Approach for the
1134 Development of Alternative Methods in Toxicology. *ALTEX*, 42.
1135 <https://doi.org/10.14573/altex.2412241>
- 1136 Tanabe, S., Beaton, D., Chauhan, V., Choi, I., Choi, J., Clerbaux, L.-A., Coppola, L., Dumont,
1137 A. F., Esterhuizen, M., Filipovska, J., FitzGerald, R., Fritsche, E., Garcia-Reyero, N.,
1138 Goralczyk, A., Huliganga, E., Kim, Y.-J., Klose, J., Rocca, C. L., Landesmann, B., ...
1139 Yauk, C. (2023). Report of the 3rd and 4th Mystery of Reactive Oxygen Species
1140 Conference. *ALTEX*, 689–693. <https://doi.org/10.14573/altex.2307041>
- 1141 Tanabe, S., Beaton, D., Chauhan, V., Choi, I., Danielsen, P. H., Delrue, N., Esterhuizen, M.,
1142 Filipovska, J., FitzGerald, R., Fritsche, E., Gant, T. W., Garcia-Reyero, N., Helm, J.
1143 S., Huliganga, E., Jacobsen, N. R., Kay, J. E., Kim, Y.-J., Klose, J., Rocca, C. L., ...
1144 Yauk, C. (2022). Report of the 1st and 2nd Mystery of Reactive Oxygen Species
1145 Conferences. *ALTEX*, 336–338. <https://doi.org/10.14573/altex.2203011>
- 1146 Van Ertvelde, J., Verhoeven, A., Maerten, A., Cooreman, A., Santos Rodrigues, B. D.,
1147 Sanz-Serrano, J., Mihajlovic, M., Tripodi, I., Teunis, M., Jover, R., Luechtefeld, T.,
1148 Vanhaecke, T., Jiang, J., & Vinken, M. (2023). Optimization of an adverse outcome
1149 pathway network on chemical-induced cholestasis using an artificial
1150 intelligence-assisted data collection and confidence level quantification approach.

- 1151 *Journal of Biomedical Informatics*, 145, 104465.
1152 <https://doi.org/10.1016/j.jbi.2023.104465>
- 1153 Varga, Z. V., Ferdinandy, P., Liaudet, L., & Pacher, P. (2015). Drug-induced mitochondrial
1154 dysfunction and cardiotoxicity. *American Journal of Physiology-Heart and Circulatory*
1155 *Physiology*, 309(9), H1453–H1467. <https://doi.org/10.1152/ajpheart.00554.2015>
- 1156 Verhoeven, A., Sanz-Serrano, J., & Vinken, M. (2025). Mechanism-based new approach
1157 methodologies for in vitro detection of chemical-induced liver steatosis. *Archives of*
1158 *Toxicology*. <https://doi.org/10.1007/s00204-025-04235-5>
- 1159 Verhoeven, A., Van Ertvelde, J., Boeckmans, J., Gatzios, A., Jover, R., Lindeman, B.,
1160 Lopez-Soop, G., Rodrigues, R. M., Rapisarda, A., Sanz-Serrano, J., Stinckens, M.,
1161 Sepehri, S., Teunis, M., Vinken, M., Jiang, J., & Vanhaecke, T. (2024). A quantitative
1162 weight-of-evidence method for confidence assessment of adverse outcome pathway
1163 networks: A case study on chemical-induced liver steatosis. *Toxicology*, 505, 153814.
1164 <https://doi.org/10.1016/j.tox.2024.153814>
- 1165 Villeneuve, D. L., Angrish, M. M., Fortin, M. C., Katsiadaki, I., Leonard, M.,
1166 Margiotta-Casaluci, L., Munn, S., O'Brien, J. M., Pollesch, N. L., Smith, L. C., Zhang,
1167 X., & Knapen, D. (2018). Adverse outcome pathway networks II: Network analytics.
1168 *Environmental Toxicology and Chemistry*, 37(6), 1734–1748.
1169 <https://doi.org/10.1002/etc.4124>
- 1170 Villeneuve, D. L., Crump, D., Garcia-Reyero, N., Hecker, M., Hutchinson, T. H., LaLone, C.
1171 A., Landesmann, B., Lettieri, T., Munn, S., Nepelska, M., Ottinger, M. A., Vergauwen,
1172 L., & Whelan, M. (2014). Adverse Outcome Pathway (AOP) Development I:
1173 Strategies and Principles. *Toxicological Sciences*, 142(2), 312–320.
1174 <https://doi.org/10.1093/toxsci/kfu199>

- 1175 Vinken, M., Knapen, D., Vergauwen, L., Hengstler, J. G., Angrish, M., & Whelan, M. (2017).
1176 Adverse outcome pathways: A concise introduction for toxicologists. *Archives of*
1177 *Toxicology*, 91(11), 3697–3707. <https://doi.org/10.1007/s00204-017-2020-z>
- 1178 Wickham, H. (2016). *Ggplot2*. Springer International Publishing.
1179 <https://doi.org/10.1007/978-3-319-24277-4>
- 1180 Wiklund, L., Caccia, S., Pípal, M., Nymark, P., & Beronius, A. (2023). Development of a
1181 data-driven approach to Adverse Outcome Pathway network generation: A case
1182 study on the EATS-modalities. *Frontiers in Toxicology*, 5, 1183824.
1183 <https://doi.org/10.3389/ftox.2023.1183824>
- 1184 Wittwehr, C., Audouze, K., Burgdorf, T., Clerbaux, L.-A., Coerek, E., DEMUYNCK, E.,
1185 EXNER, T., FILIPOVSKA, J., FRITSCHÉ, E., GERIS, L., HENCH, V., JELIAZKOVA,
1186 N., KARSCHNIK, T., KYCHOVSKA, E., MAIA LADEIRA, L. C., MALINOWSKA, J.,
1187 MARINOV, E., MARTENS, M., MERTENS, B., ... VIVIANI, B. (2025). *SKIG report*
1188 *2023-2024: Society for the Advancement of AOPs Knowledgebase Interest Group*.
1189 Publications Office of the European Union.
1190 <https://data.europa.eu/doi/10.2760/7749010>
- 1191 Wittwehr, C., Clerbaux, L.-A., Edwards, S., Angrish, M., Mortensen, H., Carusi, A.,
1192 Gromelski, M., Lekka, E., Virvilis, V., Martens, M., Santos, L. O. B. da S., & Nymark,
1193 P. (2023). Why adverse outcome pathways need to be FAIR. *ALTEX*.
1194 <https://doi.org/10.14573/altex.2307131>